HHS Public Access

Author manuscript

Toxicol Appl Pharmacol. Author manuscript; available in PMC 2017 October 01.

Published in final edited form as:

Toxicol Appl Pharmacol. 2016 October 1; 308: 32–45. doi:10.1016/j.taap.2016.08.013.

Phenotypically anchored transcriptome profiling of developmental exposure to the antimicrobial agent, triclosan, reveals hepatotoxicity in embryonic zebrafish

Derik E. Haggard[1], **Pamela D. Noyes**[1,2], **Katrina M. Waters**[3], and **Robert L. Tanguay**[1,*]

[1]Department of Environmental and Molecular Toxicology, Oregon State University, Corvallis, OR

[2]Office of Science Coordination and Policy (OSCP), Office of Chemical Safety and Pollution Prevention, U.S. Environmental Protection Agency, Washington, DC

[3]Biological Sciences Division, Pacific Northwest National Laboratory, Richland, WA

Abstract

Triclosan (TCS) is an antimicrobial agent commonly found in a variety of personal care products and cosmetics. TCS readily enters the environment through wastewater and is detected in human plasma, urine, and breast milk due to its widespread use. Studies have implicated TCS as a disruptor of thyroid and estrogen signaling; therefore, research examining the developmental effects of TCS is warranted. In this study, we used embryonic zebrafish to investigate the developmental toxicity and potential mechanism of action of TCS. Embryos were exposed to graded concentrations of TCS from 6–120 hours post-fertilization (hpf) and the concentration where 80% of the animals had mortality or morbidity at 120 hpf (EC_{80}) was calculated. Transcriptomic profiling was conducted on embryos exposed to the EC_{80} (7.37 μM). We identified a total of 922 significant differentially expressed transcripts (FDR adjusted p-value ≤ 0.05; fold change ≥ 2). Pathway and gene ontology enrichment analyses identified biological networks and transcriptional hubs involving normal liver functioning, suggesting TCS may be hepatotoxic in zebrafish. Tissue-specific gene enrichment analysis further supported the role of the liver as a target organ for TCS toxicity. We also examined the *in vitro* bioactivity profile of TCS reported by the ToxCast screening program. TCS had a diverse bioactivity profile and was a hit in 217 of the 385 assay endpoints we identified. We observed similarities in gene expression and hepatic steatosis assays; however, hit data for TCS were more concordant with the hypothesized CAR/PXR activity of TCS from rodent and human *in vitro* studies.

*Correspondence to: Robert Tanguay, Ph.D. Department of Environmental and Molecular Toxicology, the Sinnhuber Aquatic Research Laboratory 28645 East Highway 34, Oregon State University, Corvallis, OR 97333. Robert.Tanguay@oregonstate.edu, Telephone: 1-541-737-6514, Fax: 1-541-737-6074.

The authors have no conflicts of interest to declare.

Keywords

Triclosan; Zebrafish; Transcriptomics; Phenotypic anchoring; Hepatotoxicity; ToxCast

Introduction

Triclosan (TCS) is a commonly used antimicrobial agent found in many personal care products including hand soaps, toothpastes, various cosmetics, textiles, and some plastics. TCS enters the environment through the general use and disposal of TCS-containing products, and is commonly found in wastewater effluent. Incomplete removal of TCS from wastewater treatment plants, and use of biosolids as soil amendments, results in the release of TCS into aquatic and terrestrial environments (Andrade *et al.*, 2015; Barber *et al.*, 2015; Davis *et al.*, 2015; Dhillon *et al.*, 2015; Kerrigan *et al.*, 2015). Due to its prevalence in many consumer products, a large proportion of humans are directly exposed to TCS. In urine samples collected by the National Health and Nutrition Examination Survey in 2003–2004, TCS was detected in 74.6% of samples from adults and children 6 years or older with a range of 2.3–3790 μg/L, which was attributed to differing degrees of elective use of TCS-containing products (Calafat *et al.*, 2008). Additionally, TCS has been detected in both adult and infant blood and breast milk, increasing concern for potential risk to human development (Allmyr *et al.*, 2006; Calafat *et al.*, 2008; Pycke *et al.*, 2014; Arbuckle *et al.*, 2015; Azzouz *et al.*, 2016; Han *et al.*, 2016).

Efforts among regulatory agencies seek to gain a better understanding of potential hazards from chemicals that are prevalent in the environment or that lack safety information. Leading this effort is the US Environmental Protection Agency National Center for Computational Toxicology's Toxicity Forecaster screening program (ToxCast) (Dix *et al.*, 2007). ToxCast provides comprehensive high-throughput bioactivity data across a wide spectrum of toxicological and biological pathways and was developed to screen and prioritize thousands of chemicals; identifying those that pose the most hazard to human health and the environment for more testing. As part of the ToxCast program, a population-based *in vitro-to-in vivo* extrapolation model was developed to estimate oral equivalent doses (OED) for 35 environmental chemicals, including TCS (Rotroff *et al.*, 2010). Only TCS and one other chemical from this screen had equivalent doses (average OED of three ToxCast assays: 0.0096 mg/kg/day) that overlapped with estimated chronic aggregate human exposure levels (0.13 mg/kg/day). Due to the concerns about human exposure, bioactivity, and potential unknown developmental effects, the use of TCS in consumer products has come into question. The FDA is currently evaluating the safety and efficacy of TCS (Bergstrom, 2014; Kuehn, 2014), the state of Minnesota recently banned the sale of TCS-containing products beginning in 2017, and several companies (including Johnson & Johnson, Colgate-Palmolive, and Avon) have or are in the process of removing TCS from their products.

Concerns have been raised about the potential for TCS to perturb endocrine functioning given the structural similarities of TCS to thyroid hormones and some estrogens. In terms of thyroid bioactivity, studies in amphibians have shown that exposure to TCS accelerates

thyroid hormone-dependent metamorphosis and alters expression of several amphibian thyroid hormone-dependent biomarker genes, including increases in proliferating cell nuclear antigen and decreases in thyroid receptor beta (Veldhoen *et al.*, 2006; Marlatt *et al.*, 2013). In contrast, exposures to TCS caused a dose-dependent decrease in total serum thyroxine (T4) levels in rats at various life stages (Crofton *et al.*, 2007; Zorrilla *et al.*, 2009; Paul *et al.*, 2010a; Paul *et al.*, 2010b; Stoker *et al.*, 2010; Paul *et al.*, 2012; Axelstad *et al.*, 2013). It has been hypothesized that TCS decreases serum T4 through increased hepatic catabolism mediated by activation of the constitutive androstane receptor (CAR) and/or pregnane X receptor (PXR) xenobiotic metabolism pathways (Crofton *et al.*, 2007). Activation of these receptor pathways leads to upregulation in phase I and II enzymes including several cytochrome P450s, sulfotransferases, and UDP-glucuronosyltransferases (UGTs) which enhances the elimination of circulating T4 by the liver. Indeed, TCS activated the human PXR and differentially affected human CAR isoforms (Jacobs *et al.*, 2005; Paul *et al.*, 2013). Furthermore, *in vivo* studies in rats exploring this hypothesis have shown transcriptional activation of *Cyp2b* and *Cyp3a*, and increased PROD and UGT enzymatic activity (Zorrilla *et al.*, 2009; Paul *et al.*, 2012). Studies that have targeted TCS estrogenic bioactivity have shown that it interacts with the ER. Although there are conflicting *in vitro* studies showing that TCS has estrogenic and anti-estrogenic activity, the majority of *in vivo* studies have demonstrated that TCS is a potential ER agonist (Ishibashi *et al.*, 2004; Ahn *et al.*, 2008; Gee *et al.*, 2008; Stoker *et al.*, 2010; Huang *et al.*, 2014; Yueh *et al.*, 2015; Yueh and Tukey, 2016). TCS increased hepatic vitellogenin gene expression in adult male medaka (Ishibashi *et al.*, 2004), as well as led to precocious puberty in female rats and enhanced the effects of ethinyl estradiol in a rat pubertal study and uterotrophic assay, respectively (Stoker *et al.*, 2010; Louis *et al.*, 2013). TCS also increased estrogen response element luciferase activity in transfected rat pituitary GH3 cells (Jung *et al.*, 2012). In the same study, three-day exposures to TCS significantly increased uterine weight, C3 expression, and uterine *CaBP-9k* expression in immature rats (Jung *et al.*, 2012). Collectively, these data suggest that TCS disrupts endocrine activity, and more research is needed to fully elucidate the mechanisms of the observed endocrine effects.

The zebrafish is an ideal *in vivo* model for studying the developmental and reproductive toxicity of chemicals. It's rapid, external development and transparency make it amenable to high-throughput chemical screens examining a wide range of biological endpoints (Padilla *et al.*, 2012; Truong *et al.*, 2014; Noyes *et al.*, 2015). Zebrafish share high genetic homogeneity to humans, with 71% of human genes having an ortholog (Howe *et al.*, 2013), and many developmental and biological signaling pathways conserved between zebrafish and humans. The effects of TCS have previously been studied in both the developing and adult zebrafish (Tatarazako *et al.*, 2004; Oliveira *et al.*, 2009; Padilla *et al.*, 2012; Truong *et al.*, 2014; Chen *et al.*, 2015). Dietary exposure of adult zebrafish to TCS for 21 days resulted in hyperplasia of thyroid tissues, with increased thyroid follicle size and number, and increased mRNA expression of the thyroid sodium-iodide symporter (NIS) and thyroid-stimulating hormone (TSH) (Pinto *et al.*, 2013). Developmental exposure to TCS caused changes in lipid droplet accumulation and decreased the expression of several transcripts involved in β-oxidation of fatty acids in larval zebrafish (Ho *et al.*, 2016). However, to our knowledge, no studies have taken a global, transcriptomic approach to examine the possible mechanism of the

developmental toxicity of TCS in zebrafish. Whole-genome transcriptomics in embryonic zebrafish represents an untargeted, unbiased method to investigate putative mechanisms of action for various compounds, as the full repertoire of the genome is expressed over the course of development. Transcriptomic studies of 48 hpf embryos have identified differential mechanisms and upstream transcriptional regulation after exposure to phenotypically anchored concentrations of polycyclic aromatic compounds and their oxygenated derivatives (Goodale *et al.*, 2013; Goodale *et al.*, 2015). Similarly, transcriptomic analysis of select estrogenic and anti-estrogenic compounds detected disruption of several distinct endocrine-related biological pathways, supporting the use of 48 hpf embryos in a mechanistic context to identify potential endocrine disrupting compounds (Schiller *et al.*, 2013). For these reasons, we hypothesized that transcriptomics at 48 hpf would provide meaningful insight into the mechanism of TCS developmental toxicity in zebrafish and provide information regarding the endocrine disrupting potential of TCS.

Herein, we used a phenotypically anchored toxicogenomics approach to investigate the mechanism of toxicity after developmental exposure of embryonic zebrafish to TCS. Zebrafish were exposed from 6–120 hpf to TCS to identify the concentration at which 80% of exposed embryos have an adverse effect (EC_{80}) in our model system, and whole-genome transcriptomics was conducted using high-density microarrays to examine the effects of TCS on the 48 hpf zebrafish transcriptome. TCS exposure induced robust transcriptional changes with a majority of transcripts being significantly decreased. Downstream functional analysis of the transcriptional responses indicated disruption of many processes related to normal liver functioning, but no responses that would indicate disruption of thyroid or estrogen signaling at the early developmental life-stage tested.

Methods

Chemicals

Triclosan (CAS: 3380-34-5; 99.7%) was obtained from Sigma Aldrich (catalog number PHR1338), and stock solutions were prepared in dimethyl sulfoxide (DMSO; Avantor Performance Materials, Center Valley, PA) at a concentration of 10 mM. For all experiments, the maximum DMSO percentage for all exposure concentrations, including control exposures, was 0.64%.

Zebrafish husbandry

Wild-type 5D zebrafish were used for all experiments. Zebrafish were maintained at the Sinnhuber Aquatic Research Laboratory on a 28°C recirculating water system with a 14:10 hour light/dark photoperiod. Embryos were collected in the morning from group spawns of adult zebrafish. In brief, large group tanks of adult zebrafish with a 1:1 male female ratio were set up one day prior to spawning. In the morning, embryos were collected from the tanks using an internal collection apparatus. Embryos were cleaned, age staged in spans of no more than one hour, and kept in petri dishes under the same conditions as adults prior to chemical exposure (Kimmel *et al.*, 1995). Animal handling and use were conducted according to Institutional Animal Care and Use Committee procedures at Oregon State University.

TCS exposure

At six hours post-fertilization, the chorions were removed and the embryos placed, one embryo per well, in 96-well microplates pre-filled with 100 μL embryo medium using our automated dechorionator and embryo placement systems (Mandrell *et al.*, 2012). For all experiments, TCS stocks were dispensed to each well using the HP D300 Digital Dispenser and subsequently normalized to 0.64% DMSO (HP Development Company, L.P., Vancouver, WA). For the initial developmental toxicity studies, zebrafish were exposed under static conditions to nominal concentrations of 1, 4, 6, 8 and 10 μM TCS in 0.64% DMSO or the 0.64% DMSO control for 6–120 hpf (n = 32 embryos per exposure concentration). Mortality and morbidity were assessed at 24 and 120 hpf using a suite of 22 endpoints as previously described (Truong *et al.*, 2011). As adverse morphological effects in zebrafish provide little direct mechanistic information regarding a chemical's toxicity and are often correlated with one another (Truong *et al.*, 2014), we consolidated the mortality and morbidity data into an "effect" or "no effect" response across all exposure groups. As a result, each animal was assigned either a 1 or a 0 depending on whether it had any mortality/morbidity or had no adverse effect, respectively. Logistic regression analysis was performed (using the *glm* function for the binomial family with the logit model link function in R), and the EC_{80} was calculated based on the logistic curve using the *dose.p* function in R (R Core Team, 2013). For the microarray experiment, embryos were exposed to 0 or 7.37 μM TCS (the calculated EC_{80}) from 6–48 hpf and RNA was isolated as described below. As the original chemical stock of TCS expired over the course of these studies after the microarray data had been collected, we repeated the EC_{80} experiment with a new chemical stock of TCS at 1, 2, 3, 4, 5, 6, 7, 8, 9, and 10 μM TCS in 0.64% DMSO or the 0.64% DMSO control following the same exposure conditions and data analyses described above. For the EC_{80} time course study, embryos were exposed to 0 μM of 6.46 μM from 6–120 hpf. There were a total of 33 embryos in the 0 μM group and 143 embryos in the 6.46 μM group for this study. Mortality and morbidity were assessed at 24, 48, 72, 96, and 120 hpf. Images at each life stage were taken using the Keyence BZ-X710 fluorescent microscope (Keyence, Osaka, Japan).

RNA isolation

RNA was isolated from groups of eight 48 hpf embryos using the Zymo Quick-RNA MiniPrep kit (Irvine, CA) for the microarray study or the Zymo Direct-zol RNA MiniPrep kit (Irvine, CA) for the qRT-PCR studies. Embryos were homogenized in 300 μl lysis buffer for microarray samples or 500 μl RNAzol RT (Molecular Research Center, Cincinnati, OH) for the qRT-PCR samples with 0.5 mm zirconium oxide beads using a bullet blender (Next Advance, Averill Park, NY) for 3 minutes at speed 8. RNA was extracted according to the manufacturer's protocols. The optional in-column DNase I digestion step was performed for the microarray samples. Total RNA concentration and quality was determined on a SynergyMX spectrophotometer using the Gen5 Take3 system (BioTek Instruments, Inc., Winooski, VT).

Microarray processing

RNA was isolated from groups of 8 pooled embryos as described above with four biological replicates per treatment group. RNA integrity was determined using the Agilent 2100 Bioanalyzer (Agilent Technologies, Santa Clara, CA), with an allowable minimum RIN score of 7. Aliquots of 600 ng total RNA for each sample were placed in RNAstable® tubes (Biomatrica, San Diego, CA) and dried according to the manufacturer's instructions for shipment to OakLabs GmBH (Hennigsdorf, Germany) for processing on ArrayXS Zebrafish microarrays. Each array contains oligonucleotides for 48,370 coding and 8,075 non-coding sequences that are sourced from Ensembl ZV9 release 75. Upon arrival at the processing facility, samples were re-hydrated and the Low Input Quick Amp WT Labeling Kit (Agilent Technologies) was used to generate cyanine 3-CT labeled cRNA according to the manufacturer's protocols. Samples were hybridized to ArrayXS Zebrafish microarrays using the Gene Expression Hybridization Kit (Agilent Technologies). Fluorescent signals on the microarrays were detected using the SureScan Microarray Scanner (Agilent Technologies). After scanning, the image files were read and processed using Agilent Feature Extraction software (version 11) and raw data was provided for further in-house processing and analysis.

Microarray analysis

Data filtering, background correction, normalization, and statistical analyses were performed in R using the *limma* Bioconductor package (Smyth, 2004; Ritchie *et al.*, 2015). Arrays were first background corrected using the maximum likelihood estimation method and then quantile normalized (Silver *et al.*, 2009). Prior to linear modeling and differential expression calculation, control probes and any probe that was less than 10% brighter than the negative control probes on at least four of the arrays were filtered from the analysis. Raw and normalized microarray data were uploaded to the Gene Expression Omnibus and are publically available (GSE80955). Differential expression testing was performed in *limma* by fitting the data to a simple linear model, estimating the moderated standard errors using the empirical Bayes method, resulting in the calculation of moderated t-statistics for each gene. P-values were adjusted using a 5% false discovery rate (FDR) using the Benjamini-Hochberg procedure. Transcripts with adjusted P-value ≤ 0.05 and a $\log_2$ fold-change ± 2.0 were considered significantly differentially expressed. Visualization of gene expression profiles were generated in R using heatmap.2 with bi-directional hierarchical clustering of the significant differentially expressed transcripts. We identified enriched Gene Ontology (GO) terms of the significantly increased and decreased transcript sets using the Database for Annotation, Visualization and Integrated Discovery (DAVID) Bioinformatics Resources 6.7 tool (Huang da *et al.*, 2009b; Huang da *et al.*, 2009a). Ensembl zebrafish transcript identifiers were used for DAVID analysis, and included the annotated array transcriptome as the reference background. We considered GO terms for Biological Process at levels 3, 4, or 5 and applied the high classification stringency setting for analysis. DAVID uses an adjusted Fisher's exact test (EASE) to determine enriched GO terms within a given significant differentially expressed gene set compared to the reference background set. Functional annotation clustering was performed on the enriched GO terms to reduce redundancy and group related ontologies into more functional categories. Enriched GO terms with a P-value ≤ 0.05 in the functional clusters were considered significant. Since each cluster consisted of

multiple enriched GO terms, and included significant and non-significant GO terms, the consensus significant GO term for each cluster are reported, as we have done previously (Tilton *et al.*, 2015).

Pathway analysis

Since the ArrayXS Zebrafish platform uses Ensemble zebrafish transcript identifiers, we identified all orthologous human Ensembl gene identifiers using Ensembl BioMart (http://www.ensembl.org/biomart/) based on the Zv9 (release 75) transcriptome and the Bioinformatics Resource Manager v 2.3 prior to pathway analysis (Tilton *et al.*, 2012; Flicek *et al.*, 2014). Of the 60,022 total unique probes, we were able to identify 41,143 orthologous human Ensembl gene identifiers (~69% mapping efficiency), 14,929 of which were unique. To better understand the functional consequences of TCS exposure, and to relate the observed transcriptional changes to human health and disease outcomes, we performed biological process network enrichment analysis and transcription factor prediction using MetaCore GeneGo software. Enrichment statistics are based on a hypergeometric distribution, where the P-value is the probability that transcripts in a differentially expressed gene set that map to a curated biological process, or are under regulation by a transcription factor, are overrepresented compared to the reference background set of genes, as we have done previously (Nikolsky *et al.*, 2009; Waters *et al.*, 2012). Only enriched biological process networks with a FDR-correct P-value ≤ 0.05 were considered significant. For the transcription factor analysis, predicted transcription factors with a P-value ≤ 5e-05 were considered significant.

Tissue-specific gene enrichment analysis

The orthologous human differentially expressed genes that were used in the MetaCore enrichment studies were converted to their associated gene symbol using Ensembl BioMart. After filtering for significant differential expression (adjusted P-value ≤ 0.05; fold change ≥ 2), the resulting 450 significant genes were used for tissue-specific gene enrichment analysis. We utilized the Tissue Specific Expression Analysis (TSEA) tool in order to perform tissue-specific gene enrichment analysis based on human tissue expression data (http://genetics.wustl.edu/jdlab/tsea/), which performs a Fisher's exact test with Benjamini-Hochberg correction of the overlap between a user-supplied gene list and a reference gene list at different tissue specificity thresholds (Dougherty *et al.*, 2010; Xu *et al.*, 2014; Wells *et al.*, 2015). This tool was developed from data collected as part of the Genotype-Tissue Expression project, which includes RNA-seq data from 45 different tissues collected from 189 subjects. For 25 of these tissues, every gene identified was given tissue specificity P-values (pSI), based on a tissue-specific indexing method (Dougherty *et al.*, 2010; Xu *et al.*, 2014). If a gene had a low pSI score for a specific tissue, its expression was highly enriched in that tissue compared to all other tissues. Enrichment statistics from the TSEA tool are visualized as sets of concentric hexagonal nodes, each representing a tissue type, and are hierarchically ordered as a dendrogram based on the similarity of tissue-specific genes across tissue types (described in Figure 2 of Wells, et al. (2015)). In brief, the size of the outermost hexagon of each node is proportional to the total number of tissue-specific transcripts enriched in that particular tissue. Smaller hexagons within each tissue node represent a more stringent threshold of tissue-specific expression pSI values (0.05, 0.01,

0.001, and 0.001, respectively), and are indicative of increasing degrees of tissue-specific gene sets. The color of each hexagon is related to the FDR-corrected P-value from the Fisher's exact tests of the overlap between the user-supplied differentially expressed gene list and the reference gene lists. Striped colors represent a low degree of tissue specificity in the reference gene set. A total of 450 TCS-induced differentially expressed genes were analyzed.

Quantitative real-time PCR

To provide further support that the robust gene expression response observed in the microarray study pertains to the mechanism of action of TCS, we performed quantitative RT-PCR (qRT-PCR) on fifteen significant differentially expressed genes from the microarray data at the EC_{20}, EC_{50}, and EC_{80} of TCS based on the repeated EC_{80} developmental study. Zebrafish embryos were exposed to 0, 3.62, 5.04, or 6.46 μM TCS and RNA was isolated as described above at 48 hpf. Primers for the target genes are listed in Supplementary Table 1. cDNA was generated from total RNA using the ABI High-capacity cDNA Reverse Transcription kit (Thermo Fisher, Waltham, MA) following the manufacturer's protocol. qRT-PCR was conducted in 12.5 μl reactions consisting of 6.25 μl ABI *Power* SYBR Green PCR Master Mix (Thermo Fisher), 3.25 μ Hl_2O, 0.5 μl of each primer, and 2 μl of cDNA (12.5 ng/μl) using the StepOnePlus Real-Time PCR system (Thermo Fisher). Cycling conditions were used according to manufacturer's instructions. Fold-change measurements relative to control samples were calculated using the method described in Pfaffl (Pfaffl, 2001), using β-actin for normalization. Four biological replicates per treatment group were used for qRT-PCR studies. Data were statistically analyzed in R using a one-way ANOVA with Tukey post-hoc test or the Kruskal-Wallis test with Dunn's post-hoc test for data that passed or failed normality testing, respectively. We qualitatively compared the microarray and the qRT-PCR data by taking the $\log_2$ fold-change value for probes that mapped to the same Ensembl zebrafish gene ID from the microarray and the average fold change value from the qRT-PCR study. qRT-PCR data and statistics are provided in Supplementary Table 2.

ToxCast *in vitro* bioactivity data analysis

TCS was part of the ToxCast phase I chemical library, and *in vitro* bioactivity data are publicly available for this chemical across a large number of screening assays. To our knowledge, data from this program represent the most comprehensive *in vitro* bioactivity assessment of TCS. As such, we were interested in examining the bioactivity profile of TCS across ToxCast to determine whether there were similarities in responses with our transcriptomic analysis in terms of gene expression signatures and predicted transcription factor activities. All of the ToxCast bioactivity data for TCS was downloaded from the interactive Chemical Safety for Sustainability dashboard (iCSS; http://actor.epa.gov/dashboard/#chemical/3380-34-5; prod_dashboard_v2) (USEPA, 2015). Only bioactivity data from assays that were tested at three or more concentrations were used. Data were filtered based on background control assays, assay endpoints in which the detected signal direction (gain/loss) was not developed or validated for that specific assay. Since we are interested in hit percentages rather than calculated AC_{50} values, for assays in which there was a positive hit-call in only one statistical model, we retained the data for the positive hit-call only. In the

case where data for an assay had no hit-call or was a hit for both models, we retained only the first instance of that assay. The ToxCast assays are organized by different annotation terms which contain specific information about each assay including manufacturer, cell type used, assay detection technology, biological process, and intended target family (e.g. cytokine, nuclear receptor, etc.). The positive hit-call data for TCS were visualized based on three annotation levels defined by the ToxCast program: biological process target, intended target family, and nuclear receptors from the intended target family annotation level. Data were visualized using a radial pie chart using custom R code and the plotrix package (Lemon, 2006). We only report assay data that had a positive hit for each annotation level. However, all data are available in the supplement (Supplementary Table 3, 4, and 5).

Results

Evaluating the developmental toxicity of TCS and computing an EC_{80}

Developmental exposure to 8 and 10 μM TCS resulted in a high prevalence of 24 hpf developmental delay (DP24) followed by 120 hpf mortality (MORT; Figure 1A). Exposure to 1, 4, and 6 μM TCS was not associated with mortality but resulted in a variety of malformations including jaw, axial, caudal fin, pectoral fin, eye, jaw, snout, yolk sac edema, and pericardial edema defects with a total percent prevalence of 12.5%, 28.1%, and 40.6%, respectively, for any adverse effect (Figure 1A). We identified the concentration of TCS associated with an 80% incidence of morphological and mortality effects to be 7.37 μM, which was used in the gene expression studies described below (Figure 1B; EC_{80} indicated by dashed lines). Since we are pooling larvae for RNA collection before they display the full range of endpoints, it is critical to ensure that the selected TCS concentration used for transcriptome analysis results in a large majority of the larvae being affected three days later. This increases the probability that the gene expression changes measured will be causally related to later adverse responses. It was also important to use a high effect concentration in an attempt to maximize the transcriptional signal-to-noise ratio, which can be problematic when using fluorescence intensity-based microarray technologies. Selecting too low a concentration for the array study (e.g. an EC_{10} or EC_{20}) would mean that we would be measuring the expression levels from mostly normal, unaffected fish. As a result, it would be more difficult to observe strong transcriptional signatures indicative of an effect as it would be masked by the expression profiles of embryos within that concentration group that are unaffected by the exposure.

Transcriptome profiling of TCS exposure

A total of 2646 transcripts were significantly differentially expressed after exposure to TCS compared to control (FDR-adjusted P-value ≤ 0.05). For downstream functional analysis, we focused only on transcripts with a fold change ≥ 2.0. This filtering resulted in 165 and 757 elevated or repressed transcripts, respectively. To visualize the expression profile, we generated a heatmap with bi-directional hierarchical clustering to see the treatment differences as well as clustering of similarly differentially expressed transcripts (Figure 2). TCS exposure produced a strong transcriptional profile, highlighted by the separation of the TCS-treated and control replicates, with two primary transcript clusters that reflected either increased or decreased differential expression. Transcripts within the significantly increased

cluster were associated with nucleosome assembly processes, whereas the cluster of decreased transcripts consisted of transcripts involved in oxygen transport, hypoxia, blood coagulation, platelet activation, hexose metabolism, glycolysis, nucleic acid biosynthesis or metabolism, and eye morphogenesis (Figure 2).

Pathways analysis of TCS

Of the 922 significantly differentially expressed transcripts with a fold change ≥ 2.0 from the microarrays, we were able to identify 476 unique human orthologous genes using a combination of Ensembl BioMart and the Bioinformatics Resource Manager software. As shown in Table 1, we observed several significantly enriched processes involved in immune system development such as the Kallikrein-kinin and complement systems, and IL-6 signaling pathways. TCS exposure also affected processes involved in insulin signaling, blood coagulation, bile acid regulation of lipid metabolism and negative FXR-dependent regulation of bile acids concentration, visual perception, and synaptic vesicle exocytosis processes. To identify any potential regulators of the observed transcriptional changes induced by exposure to TCS, we also performed transcription factor prediction analysis. A total of 16 transcription factors were predicted to regulate many of the significant differentially expressed transcripts affected by developmental exposure to TCS ($p \leq 5e\text{-}05$; Table 2). Four hepatocyte nuclear factor (HNF) transcription factors were predicted to be involved in the transcriptional profile of TCS, all of which have been demonstrated to regulate a large number of liver-enriched transcripts in zebrafish (Cheng *et al.*, 2006).

TCS transcripts are predicted to be enriched in the liver and brain

We performed tissue-specific gene set enrichment analysis to identify potential tissue-specific transcriptional responses, which may be indicative of TCS target organ/tissue toxicity, using the publicly available TSEA tool. As shown in Figure 3, transcripts significantly differentially expressed by TCS exposure were shown to be highly enriched in the liver and brain. We also observed moderate transcriptional enrichment in muscle, heart, kidney, pituitary, and pancreas. However, there was no significant enrichment at more stringent specificity thresholds for these tissues. No significant enrichment in thyroid or reproductive tissues, such as the ovary or testis, was observed.

Developmental toxicity time course at the TCS EC_{80}

As a result of the TCS stock used for the original developmental toxicity assessments and microarray study expiring, we repeated the initial EC_{80} developmental toxicity study using a new TCS chemical stock (Figure 4A). The EC_{20}, EC_{50}, and EC_{80} for the new TCS stock was 3.62, 5.04, and 6.46 μM, respectively. Exposure to TCS resulted in a similar mortality and morbidity response compared to the initial study (Supplementary Figure 1). Exposure to the new EC_{80} resulted in a prevalence of any effect at 45%, 87%, 88%, 89%, and 90% at 24, 48, 72, 96, and 120 hpf, respectively. We observed a maximum mortality in 38% of the exposed embryos by 120 hpf, and morbidity in 52% by 120 hpf which was predominated by axial defects, pericardial edema, yolk-sac edema, and caudal fin malformations (Figure 4B and C; Supplementary Figure 2).

qRT-PCR validation and gene expression concentration response of TCS

We selected fifteen genes that were significantly affected by TCS from the microarray study using qRT-PCR for validation and to determine whether the observed gene signatures are present at lower exposure concentrations. As shown in Figure 5, exposure to the EC_{80} and EC_{50} of TCS resulted in significant expression changes similar to what was observed in the microarray study for five genes and included *tfa, matn1, apoba, hp*, and *rorab*. We also observed similar expression responses for *rbp2b, fabp10a, mknk2b, atf5b, notch1a*, and *igfbp1a*; however, these effects were only observed in the EC_{80} exposure group. We did not observe any significant gene expression changes at the EC_{20} for TCS.

ToxCast *in vitro* bioactivity profile of TCS

TCS was part of ToxCast phase I chemical library, and *in vitro* bioactivity data are publicly available for this chemical across a large number of screening assays. TCS had a positive hit-call in 217 out of 385 unique assay endpoints. The bioactivity profile of TCS across the annotation terms “biological_process_target”, “intended_target_family”, and nuclear receptor assays from the “intended_target_family” are shown in Figure 6 as radial pie diagrams where the length of the slice indicates the hit-call percentage and the angle of the slice indicates the total number of assays for a specific category term in the annotation level (e.g. cell cycle, receptor binding, protein stabilization). The “biological_process_target” annotation of ToxCast assays can be considered analogous to GO process annotations and gives a good representation of overall bioactivity patterns of a chemical. At this annotation level, TCS was highly active in assays involved in the regulation of gene expression, cell-specific assays (e.g. cell death, cell cycle, cell proliferation), and was moderately active in the receptor binding and regulation of transcription factor activity assays (Figure 6A). It is important to note that the assays measuring the regulation of gene expression, receptor binding, and regulation of transcription factor activity have the greatest coverage across the ToxCast assay space as indicated by the size and angle of their corresponding slices in the figure (Supplementary Table 3). Many assays within these three categories target specific proteins, receptors, or enzymatic activities, and offer more mechanistic information regarding a chemical’s activity compared to others such as cell proliferation or cytotoxicity. Examination of the TCS activity profile across the intended target families shows that TCS was active in all protease inhibitor, cytokine, and cell adhesion molecule assays (Figure 6B; Supplementary Table 4). TCS had a 70% hit-call rate in the cytochrome P450 assays including CYP19A1 inhibition, CYP2C9, CYP1A2, and CYP2D2. To leverage the most pertinent information about possible target pathways of TCS, we focused on assays that directly measure a chemical’s ability to act on nuclear receptors (Figure 6C). TCS had a hit-call for 24 of the 80 nuclear receptor assays, which correspond to 13 of the 36 unique nuclear receptors covered in ToxCast (Supplementary Table 5). Note that the assay coverage across the nuclear receptors is dominated by estrogen receptor 1 and androgen receptor assays. TCS was a hit in all assays for retinoic X receptor B, the peroxisome proliferator-activated receptor group, progesterone receptor, and PXR. TCS was a positive hit in 70% of the androgen receptor assays. Interestingly, TCS showed a low activity for the 13 assays targeting estrogen receptor 1. Together, these results show that TCS had a diverse bioactivity response for the overall ToxCast battery of assays and had specific interaction with several

nuclear receptors and CYP enzymes that have been hypothesized to be involved in the hypothyroxinemic effects of TCS.

Discussion

The present study used phenotypically anchored whole-genome transcriptomics to investigate the potential mechanism of action of the common antimicrobial agent, TCS. Developmental toxicity studies during the exposure window of 6–120 hpf exposure to TCS identified an EC_{80} of 7.37 μM in our model system. Exposure to the TCS EC_{80} resulted in a robust transcriptional response in 48 hpf zebrafish, predominated by significantly decreased transcripts. Functional enrichment analysis using MetaCore identified several biological processes and transcription factors with roles in liver function and neural pathways. Furthermore, tissue-specific enrichment analysis showed that the liver and brain were potential target tissues for TCS-induced transcriptional changes. We also examined the ToxCast *in vitro* bioactivity profile of TCS and found a diverse activity profile across the suite of assays, including liver related endpoints, and effects in select nuclear receptor assays which corroborate the hypothesized role of PXR in TCS-induced hypothyroxinemia in rat and human *in vitro* studies. Overall, these results highlight the potential role of TCS as a hepatotoxicant in embryonic zebrafish.

In our initial developmental toxicity assessment, we observed a relatively steep concentration-response curve from TCS exposure, where 8 μM and above caused a high prevalence of developmental delay at 24 hours followed by mortality by 5 days with minimal effects at lower concentrations (Figure 1A). However, after a reevaluation of the developmental effects of TCS, using the new chemical stock with a higher resolution concentration curve, we observed an increase in morbidity at the mid-exposure concentrations at 120 hpf (Figure 4A; Supplementary Figure 2). Other developmental toxicity studies using zebrafish have observed similar morphological effects (Oliveira *et al.*, 2009; Chen *et al.*, 2015). A zebrafish early-life stage assessment of TCS reported delayed hatching, pericardial edema, and axial defects which resulted in near-complete lethality by 120 hpf in embryos exposed to 1.73 μM TCS; however, exposure to 1.04 μM TCS resulted in no difference in morphology or mortality compared to vehicle control embryos (Oliveira *et al.*, 2009).

Phenotypic anchoring is integral to toxicogenomic studies. A common practice is to use a concentration that has been anchored to a phenotypic outcome in a known percentage of exposed animals and selecting a time point that precedes the outcome with the aim of detecting chemical-induced transcriptional changes as far upstream as possible. We selected a concentration that elicited eventual morbidity or mortality by 120 hpf, and a time point, 48 hpf, that has previously been demonstrated to provide useful mechanistic information from diverse chemical exposures (Goodale *et al.*, 2013; Schiller *et al.*, 2013; Goodale *et al.*, 2015). In this case, the use of an EC_{80} was intentionally selected because it guaranteed that a large proportion of exposed animals would have a phenotype at 120 hpf. As demonstrated in the time course study (Figure 4), the assumption that the time point used in our analysis preceded all phenotypic changes did not hold. As a result, the transcriptional changes we observed may reflect responses that are concurrent and possibly downstream of the early

initiating events for TCS but nonetheless appear involved in the TCS mode of action. Furthermore, expression data representative of more downstream responses may provide additional insight regarding organ/tissue-specific toxic responses, which might not be detected at lower concentrations.

Based on our two developmental toxicity assessments, the EC_{80} of TCS was calculated to be in the range of 6.46 and 7.37 μM, and the EC_{50} to be ~5 μM. The EC_{50} value was similar to another study in which an AC_{50} value of 2.66 μM for TCS was calculated based on a six-day zebrafish high-throughput screen of the ToxCast phase I chemicals (Padilla *et al.*, 2012). These differences between studies can likely be attributed to zebrafish strain differences, chorionation status, chemical purity and delivery methods, and static non-renewal exposures in our study versus daily renewal exposures. And although a caveat of the study presented here is that we did observe morbidity at 48 hpf with the TCS EC_{80}, it is unknown the extent to which these effects contributed to the transcriptional changes we observed. It is also important to note that these EC values represent nominal aqueous concentrations and not body burden levels, as we did not directly measure TCS levels in our exposed animals. As such, the TCS exposure concentrations used at 48 hpf and throughout these studies do not equate to human doses and, therefore, provide no direct dose-response information between zebrafish and human exposures.

Exposure to TCS at the determined EC_{80} concentration elicited a robust transcriptomic response in 48 hpf zebrafish embryos, with a majority of the differentially expressed transcripts significantly decreased. Functional analysis of the two primary clusters shown in the heatmap using DAVID highlighted several biological processes that appear to be involved in liver function, namely blood coagulation, platelet activation, glycolysis, and oxygen transport (Figure 2). Functional enrichment analysis of the human orthologous genes of the significant differentially expressed transcripts using MetaCore further supported the hepatotoxic action of TCS through prediction of several biological processes that are involved in normal liver processes and potential toxicity (Table 1). The MetaCore biological pathway “regulation of metabolism—bile acid regulation of glucose and lipid metabolism via FXR”, which is directly related to the biological process network “bile acid regulation of lipid metabolism and negative FXR-dependent regulation of bile acids concentration”, was identified as the one concordant pathway in a species comparative toxicogenomics study of three hepatotoxins using embryonic zebrafish, *in vivo* and *in vitro* rodent models, and human primary hepatocytes (Driessen *et al.*, 2015). Since a large proportion of detected transcripts that were significantly differentially expressed were decreased, it is likely that these biological processes are being negatively impacted by TCS, suggesting either disruption of normal liver development or a decrease in hepatic cells responsible for these processes due to toxicity. From our transcription factor analysis, we identified several transcription factors which are known to play essential roles in liver development and may be involved in the hepatotoxic mechanism of TCS in zebrafish (Table 2). Four HNF transcription factors were predicted to play a regulatory role in the TCS transcriptional profile. HNF transcription factors are liver-enriched transcription factors that regulate, and often co-regulate, the constitutive expression of many genes crucial for liver function (Cheng *et al.*, 2006). For example, *fabp10a*, which was significantly decreased in the microarray and qRT-PCR studies at the TCS EC_{80}, has *hnf1*α and *hnf3*β consensus binding sites in a regulatory region

435-bp upstream of the promoter in zebrafish (Her *et al.*, 2003). HNF4α, the most significantly predicted transcription factor in this study, has also been shown to regulate HNF1α expression, and therefore, indirectly affects the downstream activation of HNF1α gene targets (Jung and Kullak-Ublick, 2003). Importantly, prospero homeobox protein 1, PROX1, was also predicted to have a functional role in TCS-mediated transcriptional changes. PROX1 plays an important role in early liver development and has been demonstrated to negatively regulate both HNF4α and RORα (Song *et al.*, 2006; Takeda and Jetten, 2013). This suggests that TCS exposure may be impacting the developing liver either through a potential interaction between TCS and PROX1 resulting in decreased transcriptional activation of many important target genes in the liver, mediated by repression of liver-enriched transcription factors, or by decreasing the number of hepatoblasts through an undefined toxic mechanism. Additionally, using a freely available tissue-specific gene enrichment analysis tool, we found that the TCS-induced transcriptional changes in 48 hpf zebrafish embryos are specifically enriched in the liver and brain, providing further evidence of target organ toxicity (Figure 3).

As highlighted above, functional and tissue-specific analysis of the TCS-induced gene changes involve some integral process or regulatory mechanism involved in the normal function and development of the liver. The strong repressive transcriptional signal observed in the array study would suggest that TCS exposure is causing liver developmental arrest or is directly toxic to developing hepatocytes. Indeed, many of the transcripts that were significantly decreased by TCS have been demonstrated to be reliable biomarkers of hepatotoxicity in zebrafish, including *tfa*, *fabp10a, cp, rbp2b, rbp2a*, and *apoba* (Zhang et al., 2014; Verstraelen et al., 2016). Similarly, the genes that were significantly increased due to TCS exposure have also been implicated in hepatotoxicity and liver disease/damage, including *igfbp1a, notch1a*, and *atf5b*. Induction of *igfbp1a* is a potential biomarker of hepatotoxicity and alcohol-induced liver disease, and may reflect alterations in the growth hormone-insulin-like growth factors axis or general metabolic abnormalities as a result of impaired liver function (Donaghy *et al.*, 1995; Li *et al.*, 2013; Buness *et al.*, 2014). Notch signaling is involved in the development of several organ systems, including intrahepatic biliary duct formation in the liver of mammals, performing a similar function in zebrafish (Lorent *et al.*, 2010). Notch genes play a role in the regenerative capacity of the liver and are increased in response to liver injury to induce proliferation or differentiation of the various cell types in the liver such as hepatocytes and biliary cells (Geisler and Strazzabosco, 2015). *atf5b* is a liver-enriched transcription factor, which was shown to induce CYP2B6 expression via cooperation with CAR after induction of endoplasmic reticulum stress in human hepatoma cells (Pascual *et al.*, 2008). Importantly, the qRT-PCR studies revealed that even at the EC_{50} level of exposure for five of these genes including *tfa, hp, apoba, matn1*, and *rorab* were similarly repressed, further supporting the hypothesis that TCS is negatively impacting liver function or development (Figure 5). *tfa* is an iron-binding serum protein synthesized in the liver and yolk-sac of zebrafish and is responsible for the transport of ferric iron to developing erythrocytes. Transgenic zebrafish bearing a mutation in *tfa* develop severe anemic and have decreased iron levels in somites and the gut leading to eventual embryonic mortality, suggesting its requirement for hemoglobin production (Fraenkel *et al.*, 2009). Similarly, *hp* is a globin binding protein synthesized in the liver involved in the recycling of

free serum hemoglobin. Although increases in *hp* levels are commonly associated with liver inflammation, decreases in its expression are indicative of hemolysis or potential liver damage, such as cirrhosis (Kormoczi *et al.*, 2006). Apolipoproteins, including *apoba*, are lipid transporting proteins synthesized in the liver. Decreased levels of apoliproproteins are commonly associated with primary liver cancers, cirrhosis, and chronic liver disease (Shah and Desai, 2001; Irshad and Dubey, 2005). Matrilin 1, *matn1*, is a component of basement membranes and has been shown to aid in collagen secretion. The role of *matn1* expression and liver function is unknown; however, transient knockdown of *matn1* resulted in axial, eye, and craniofacial defects which may explain, in part, the malformations observed in our developmental studies (Figure 4C; (Neacsu *et al.*, 2014). The retinoic acid-related orphan receptor, *rorab*, plays a role in the circadian regulation of lipid metabolism and is expressed in a variety of tissues including the liver, kidney, thymus, brain, and skeletal muscle (Solt *et al.*, 2011). Taken together, the observed decreases in these genes, and others, at the EC_{80} or EC_{50} of TCS demonstrate impaired liver functioning in developing zebrafish, in which prolonged disruption may result in deficiencies in iron homeostasis, anemia due to decreased hemoglobin production or hemolysis, lipid transport defects, metabolic abnormalities, and decreases in the production of critical serum proteins that are produced by the liver. Furthermore, the increased expression of several target genes, including those highlighted in the qRT-PCR study, may represent a homeostatic response of the developing liver to TCS-induced toxicity in order to maintain proper liver development and repair mechanisms (e.g. *notch1a* signaling), metabolism, and excretion of TCS by activation of xenobiotic metabolizing enzymes. These data also provided evidence that the liver bud in 48 hpf zebrafish is beginning to express a variety of genes involved in mature liver function prior to the outgrowth phase of liver development, suggesting that many of these genes are required for development. We must acknowledge the possibility that the strong transcriptomic response elicited by TCS may be a result of systemic toxicity at the EC_{80} and not indicative of target organ toxicity involving the liver and, to a lesser extent, the brain. However, the 48 hpf transcriptomic analysis presented here cannot directly differentiate between these toxic mechanisms. We reason that the functional specificity of the transcriptional changes, along with the enriched tissue expression pattern elicited by TCS, indicate systemic toxicity is not occurring. Overall, the results of our phenotypically anchored toxicogenomics analysis show that the developmental toxicity of TCS in embryonic zebrafish appears to target the developing liver and may be acting as a hepatotoxicant; however, further studies are needed to fully elucidate the mechanism by which this occurs.

Relatively few studies have focused on understanding the toxicity and endocrine effects of TCS in developing organisms, with a majority of those focusing on thyroid signaling in rats. As previously described, TCS influences thyroid-dependent metamorphosis in frogs (Veldhoen *et al.*, 2006; Marlatt *et al.*, 2013). Studies in fish have primarily focused on characterizing the acute developmental toxicity of TCS (Ishibashi *et al.*, 2004; Oliveira *et al.*, 2009; Ho *et al.*, 2016). The only mechanistic study in fish, to our knowledge, showed that five-day exposure to a no-effect concentration of TCS resulted in changes in lipid accumulation and decreased the expression of several genes involved in β-oxidation of fatty acids in zebrafish (Ho *et al.*, 2016). Interestingly, prolonged disruption of β-oxidation processes can result in microvesicular hepatocyte steatosis and eventual hepatic failure

(Cullen, 2005). In maternally exposed fetal or neonatal rats, TCS decreased serum T4 levels that then recovered to normal levels over time suggesting toxicokinetic and toxicodynamic differences between fetuses and maturing offspring (Paul *et al.*, 2010a; Paul *et al.*, 2012). However, maternally exposed offspring were still susceptible to decreases in serum T4 if directly exposed to TCS (Axelstad *et al.*, 2013). Mechanistic studies in rats investigating the role of CAR/PXR activation after maternal exposure showed that, alongside decreased serum T4 levels, TCS increased PROD activity in PND 4 animals, and although slight increases in the expression of CAR/PXR-regulated cytochrome P450 or UGT genes were detected in the dams but not the offspring, upregulated hepatic catabolism may still be a contributing factor for TCS-induced hypothyroxinemia (Paul *et al.*, 2012). In contrast to the possible role of CAR/PXR signaling in TCS-induced hypothyroxinemia as described above, our analysis of TCS-induced transcriptional changes in 48 hpf zebrafish did not identify transcriptional or downstream functional processes associated with either the thyroid or estrogen pathways as targets for TCS-induced developmental toxicity. Moreover, tissue-specific enrichment analysis showed no significant enrichment of transcripts in thyroid or reproductive tissues. We also did not observe any significant transcriptional changes in xenobiotic metabolizing enzymes that would implicate activation of the CAR/PXR signaling cascades. These included zebrafish orthologs for SULT1E1, SULT1B1, CYP2B6, CYP3A4, UGT1A1, or UGT1A6 (*sult1st3, sult1st5, cyp2y3, cyp3a65*, and *ugt1ab* respectively) nor did we observe any changes in the zebrafish PXR gene *nr1i2*. We should note that we did observe significant decreases in several *cyp2aa* family members including *cyp2aa2*, which was recently shown to be transcriptionally induced by the PXR agonists 1,4-bis [2-(3,5-dichloropyridyloxy)] benzene and phenobarbital in adult zebrafish livers (Kubota *et al.*, 2013). However, we would expect *cyp2aa2* to increase as a result of PXR activation in zebrafish, and it is likely that the observed decrease in expression was due to a decrease in the numbers of differentiating hepatoblasts/hepatocytes as a result of TCS toxicity and was not mediated through PXR. Studies of TCS in human and rodent cell-based reporter have demonstrated differential activation of CAR and PXR, where TCS activated human but not rodent PXR, and elicited various agonistic and reverse agonistic activities for CAR (Paul *et al.*, 2013). This suggests that species-specific effects may play a role in the affinity of TCS towards CAR/PXR and subsequent transcriptional activation of downstream xenobiotic metabolizing enzymes. Although, zebrafish lack a CAR gene, more research is needed to describe the effects of TCS on the zebrafish PXR (Kubota *et al.*, 2013). The lack of endocrine responses we observed in this study does not necessarily mean that TCS is incapable of endocrine disruption in zebrafish. On the contrary, studies in adult zebrafish have demonstrated TCS-induced thyroid activity (Pinto *et al.*, 2013). However, the hepatotoxic transcriptome signature of TCS we show may be specific to the window of exposure used in our studies; a potential result of immature xenobiotic sensing mechanisms in the 48 hpf liver, as it is not metabolically competent until 72 hpf (Field *et al.*, 2003). Therefore, the PXR-mediated activity of TCS would not be detected until later developmental stages, although *in situ* hybridization studies have shown that PXR mRNA is present throughout early development (Bertrand *et al.*, 2007). As such, further studies examining the transcriptomic profile of TCS across different susceptibility windows are warranted.

The activity profile of TCS across the diverse battery of ToxCast screening assays can inform and potentially corroborate the findings we present here in our zebrafish transcriptomics analysis or those posed by other laboratories. After filtering the assay data (see Methods), we found that TCS had a relatively diverse bioactivity profile and was a hit in 217 of the 385 (56.4%) assays. Assays under the biological process “Regulation of gene expression” were largely affected by TCS, and interestingly, all of these assays reported decreased transcriptional responses similar to what was observed in our array data. TCS was also a hit in two of the three “Regulation of steatosis” assays which can indicate disruption of liver metabolism. TCS bioactivity at the “intended_target_family” level highlighted unique protein classes that were affected by TCS. TCS decreased the expression of all of the cytokines within the ToxCast battery, including IL-6 which was a significantly enriched biological process network in our transcriptomic analysis. TCS was active in two of the seven FXR assays, and is likely not a direct receptor target for TCS. We also found that TCS was not a hit in the HNF4α, LXRα, LXRβ, or RORa which were predicted in our transcriptomic analysis. TCS also affected assays targeting several CYP genes regulated by CAR/PXR including human CYP2C9, CYP2C8, CYP2C19, and rat *Cyp1a2* (Tolson and Wang, 2010). Analysis of the assays targeting nuclear receptors showed that TCS was a hit in all three PXR assays and was a hit in 50% of the CAR assays, similar to that observed in previous studies (Jacobs *et al.*, 2005; Paul *et al.*, 2013). With respect to direct endocrine nuclear receptor activity, TCS had the largest activity for assays targeting the androgen receptor compared to all other endocrine receptors. Interestingly, of all the nuclear receptor assays with at least one hit-call, ESR1 was the least effected and was a hit in only 15% of ESR1-specific assays. These results show that the hit-call data for TCS across the ToxCast assays appeared to better support the hypothesized role of CAR/PXR signaling as demonstrated in human *in vitro* and rat *in vivo* studies compared to our observations and predicted functional responses of our *in vivo* transcriptomic analysis in zebrafish. This may reflect the species-dependent effects of CAR/PXR activation as previously demonstrated, or that TCS has differential mechanisms of action depending on the developmental stage resulting in presence/absence of putative molecular targets.

Collectively, these results suggest that TCS is hepatotoxic to embryonic zebrafish, and helps explain reports of acute toxicity of TCS in zebrafish and other aquatic species (Orvos *et al.*, 2002; Ishibashi *et al.*, 2004; Tatarazako *et al.*, 2004; Oliveira *et al.*, 2009; Padilla *et al.*, 2012). We demonstrated that the endocrine-related role of TCS hypothesized in rodent and human *in vitro* studies appears to not be involved in TCS-induced toxicity in zebrafish at this specific developmental stage, or was masked by the robust effects of TCS on the developing liver. Compared to the bioactivity profile of TCS across the ToxCast program, several similarities with possible liver endpoints were identified; however, the assay responses better supported the role of CAR/PXR activation by TCS in human *in vitro* systems. This may reflect biases in the assay coverage, as was demonstrated by the overrepresentation of estrogen and androgen receptor assays compared to other nuclear receptor signaling pathways. By leveraging the full repertoire of transcriptomic responses across embryonic development in the whole animal, we demonstrated that using a phenotypically anchored early developmental transcriptomics approach can inform and provide insight into putative mechanisms of chemical action. Zebrafish can not only be used to rapidly identify

phenotypic changes due to chemical exposure in a high-throughput manner (Truong *et al.*, 2014; Noyes *et al.*, 2015), it can also provide unbiased, global expression data to drive hypothesis generation about the molecular events that underlie chemical toxicity. Future studies will examine the transcriptomic response of TCS at lower concentrations and at different time points and windows of exposure to fully elucidate the role of the developing liver in TCS toxicity.

Supplementary Material

Refer to Web version on PubMed Central for supplementary material.

Acknowledgments

We would like to acknowledge Carrie Barton and Greg Gonnerman, Sinnhuber Aquatic Research Laboratory, for providing help and support with fish husbandry, spawning, and embryo screening. We would also like to thank Dr. Lisa Truong and Dr. Michael Simonich for assistance with manuscript preparation and editing. This research was supported by NIH P30 ES000210, T32 ES007060, P42 ES016465 and EPA #R835168. Pacific Northwest National Laboratory is a multi-program laboratory operated by Battelle for the U.S. Department of Energy under Contract DE-AC05-76RL01830.

Abbreviations

TCS	Triclosan
EC_{80}	80% effective concentration
EC_{50}	50% effective concentration
EC_{20}	20% effective concentration
hpf	hours post-fertilization

References

Ahn KC, Zhao B, Chen J, Cherednichenko G, Sanmarti E, Denison MS, Lasley B, Pessah IN, Kultz D, Chang DP, Gee SJ, Hammock BD. In vitro biologic activities of the antimicrobials triclocarban, its analogs, and triclosan in bioassay screens: receptor-based bioassay screens. Environ Health Perspect. 2008; 116:1203–1210. [PubMed: 18795164]

Allmyr M, Adolfsson-Erici M, McLachlan MS, Sandborgh-Englund G. Triclosan in plasma and milk from Swedish nursing mothers and their exposure via personal care products. Sci Total Environ. 2006; 372:87–93. [PubMed: 17007908]

Andrade NA, Lozano N, McConnell LL, Torrents A, Rice CP, Ramirez M. Long-term trends of PBDEs, triclosan, and triclocarban in biosolids from a wastewater treatment plant in the Mid-Atlantic region of the US. J Hazard Mater. 2015; 282:68–74. [PubMed: 25282513]

Arbuckle TE, Weiss L, Fisher M, Hauser R, Dumas P, Berube R, Neisa A, LeBlanc A, Lang C, Ayotte P, Walker M, Feeley M, Koniecki D, Tawagi G. Maternal and infant exposure to environmental phenols as measured in multiple biological matrices. Sci Total Environ. 2015; 508:575–584. [PubMed: 25483107]

Axelstad M, Boberg J, Vinggaard AM, Christiansen S, Hass U. Triclosan exposure reduces thyroxine levels in pregnant and lactating rat dams and in directly exposed offspring. Food Chem Toxicol. 2013; 59:534–540. [PubMed: 23831729]

Azzouz A, Rascon AJ, Ballesteros E. Simultaneous determination of parabens, alkylphenols, phenylphenols, bisphenol A and triclosan in human urine, blood and breast milk by continuous

solid-phase extraction and gas chromatography-mass spectrometry. J Pharm Biomed Anal. 2016; 119:16–26. [PubMed: 26637951]

Barber LB, Loyo-Rosales JE, Rice CP, Minarik TA, Oskouie AK. Endocrine disrupting alkylphenolic chemicals and other contaminants in wastewater treatment plant effluents, urban streams, and fish in the Great Lakes and Upper Mississippi River Regions. Sci Total Environ. 2015; 517:195–206. [PubMed: 25727675]

Bergstrom KG. Update on antibacterial soaps: the FDA takes a second look at triclosans. J Drugs Dermatol. 2014; 13:501–503. [PubMed: 24719072]

Bertrand S, Thisse B, Tavares R, Sachs L, Chaumot A, Bardet PL, Escriva H, Duffraisse M, Marchand O, Safi R, Thisse C, Laudet V. Unexpected novel relational links uncovered by extensive developmental profiling of nuclear receptor expression. PLoS Genet. 2007; 3:e188. [PubMed: 17997606]

Buness A, Roth A, Herrmann A, Schmitz O, Kamp H, Busch K, Suter L. Identification of metabolites, clinical chemistry markers and transcripts associated with hepatotoxicity. PLoS One. 2014; 9:e97249. [PubMed: 24836604]

Calafat AM, Ye X, Wong LY, Reidy JA, Needham LL. Urinary concentrations of triclosan in the U.S. population: 2003–2004. Environ Health Perspect. 2008; 116:303–307. [PubMed: 18335095]

Chen X, Xu B, Han X, Mao Z, Chen M, Du G, Talbot P, Wang X, Xia Y. The effects of triclosan on pluripotency factors and development of mouse embryonic stem cells and zebrafish. Arch Toxicol. 2015; 89:635–646. [PubMed: 24879426]

Cheng W, Guo L, Zhang Z, Soo HM, Wen C, Wu W, Peng J. HNF factors form a network to regulate liver-enriched genes in zebrafish. Dev Biol. 2006; 294:482–496. [PubMed: 16631158]

Crofton KM, Paul KB, Devito MJ, Hedge JM. Short-term in vivo exposure to the water contaminant triclosan: Evidence for disruption of thyroxine. Environ Toxicol Pharmacol. 2007; 24:194–197. [PubMed: 21783810]

Cullen JM. Mechanistic classification of liver injury. Toxicol Pathol. 2005; 33:6–8. [PubMed: 15805050]

Davis EF, Gunsch CK, Stapleton HM. Fate of flame retardants and the antimicrobial agent triclosan in planted and unplanted biosolid-amended soils. Environ Toxicol Chem. 2015; 34:968–976. [PubMed: 25546022]

Dhillon GS, Kaur S, Pulicharla R, Brar SK, Cledon M, Verma M, Surampalli RY. Triclosan: current status, occurrence, environmental risks and bioaccumulation potential. Int J Environ Res Public Health. 2015; 12:5657–5684. [PubMed: 26006133]

Dix DJ, Houck KA, Martin MT, Richard AM, Setzer RW, Kavlock RJ. The ToxCast program for prioritizing toxicity testing of environmental chemicals. Toxicol Sci. 2007; 95:5–12. [PubMed: 16963515]

Donaghy A, Ross R, Gimson A, Hughes SC, Holly J, Williams R. Growth hormone, insulinlike growth factor-1, and insulinlike growth factor binding proteins 1 and 3 in chronic liver disease. Hepatology. 1995; 21:680–688. [PubMed: 7533122]

Dougherty JD, Schmidt EF, Nakajima M, Heintz N. Analytical approaches to RNA profiling data for the identification of genes enriched in specific cells. Nucleic Acids Res. 2010; 38:4218–4230. [PubMed: 20308160]

Driessen M, Vitins AP, Pennings JL, Kienhuis AS, Water B, van der Ven LT. A transcriptomics-based hepatotoxicity comparison between the zebrafish embryo and established human and rodent in vitro and in vivo models using cyclosporine A, amiodarone and acetaminophen. Toxicol Lett. 2015; 232:403–412. [PubMed: 25448281]

Field HA, Ober EA, Roeser T, Stainier DY. Formation of the digestive system in zebrafish. I. Liver morphogenesis. Dev Biol. 2003; 253:279–290. [PubMed: 12645931]

Flicek P, Amode MR, Barrell D, Beal K, Billis K, Brent S, Carvalho-Silva D, Clapham P, Coates G, Fitzgerald S, Gil L, Giron CG, Gordon L, Hourlier T, Hunt S, Johnson N, Juettemann T, Kahari AK, Keenan S, Kulesha E, Martin FJ, Maurel T, McLaren WM, Murphy DN, Nag R, Overduin B, Pignatelli M, Pritchard B, Pritchard E, Riat HS, Ruffier M, Sheppard D, Taylor K, Thormann A, Trevanion SJ, Vullo A, Wilder SP, Wilson M, Zadissa A, Aken BL, Birney E, Cunningham F,

Harrow J, Herrero J, Hubbard TJ, Kinsella R, Muffato M, Parker A, Spudich G, Yates A, Zerbino DR, Searle SM. Ensembl 2014. Nucleic Acids Res. 2014; 42:D749–D755. [PubMed: 24316576]

Fraenkel PG, Gibert Y, Holzheimer JL, Lattanzi VJ, Burnett SF, Dooley KA, Wingert RA, Zon LI. Transferrin-a modulates hepcidin expression in zebrafish embryos. Blood. 2009; 113:2843–2850. [PubMed: 19047682]

Gee RH, Charles A, Taylor N, Darbre PD. Oestrogenic and androgenic activity of triclosan in breast cancer cells. J Appl Toxicol. 2008; 28:78–91. [PubMed: 17992702]

Geisler F, Strazzabosco M. Emerging roles of Notch signaling in liver disease. Hepatology. 2015; 61:382–392. [PubMed: 24930574]

Goodale BC, La Du J, Tilton SC, Sullivan CM, Bisson WH, Waters KM, Tanguay RL. Ligand-Specific Transcriptional Mechanisms Underlie Aryl Hydrocarbon Receptor-Mediated Developmental Toxicity of Oxygenated PAHs. Toxicol Sci. 2015; 147:397–411. [PubMed: 26141390]

Goodale BC, Tilton SC, Corvi MM, Wilson GR, Janszen DB, Anderson KA, Waters KM, Tanguay RL. Structurally distinct polycyclic aromatic hydrocarbons induce differential transcriptional responses in developing zebrafish. Toxicol Appl Pharmacol. 2013; 272:656–670. [PubMed: 23656968]

Han C, Lim YH, Hong YC. Ten-year trends in urinary concentrations of triclosan and benzophenone-3 in the general U.S. population from 2003 to 2012. Environ Pollut. 2016; 208:803–810. [PubMed: 26602792]

Her GM, Yeh YH, Wu JL. 435-bp liver regulatory sequence in the liver fatty acid binding protein (L-FABP) gene is sufficient to modulate liver regional expression in transgenic zebrafish. Dev Dyn. 2003; 227:347–356. [PubMed: 12815620]

Ho JC, Hsiao CD, Kawakami K, Tse WK. Triclosan (TCS) exposure impairs lipid metabolism in zebrafish embryos. Aquat Toxicol. 2016; 173:29–35. [PubMed: 26828895]

Howe K, Clark MD, Torroja CF, Torrance J, Berthelot C, Muffato M, Collins JE, Humphray S, McLaren K, Matthews L, McLaren S, Sealy I, Caccamo M, Churcher C, Scott C, Barrett JC, Koch R, Rauch GJ, White S, Chow W, Kilian B, Quintais LT, Guerra-Assuncao JA, Zhou Y, Gu Y, Yen J, Vogel JH, Eyre T, Redmond S, Banerjee R, Chi J, Fu B, Langley E, Maguire SF, Laird GK, Lloyd D, Kenyon E, Donaldson S, Sehra H, Almeida-King J, Loveland J, Trevanion S, Jones M, Quail M, Willey D, Hunt A, Burton J, Sims S, McLay K, Plumb B, Davis J, Clee C, Oliver K, Clark R, Riddle C, Elliot D, Threadgold G, Harden G, Ware D, Begum S, Mortimore B, Kerry G, Heath P, Phillimore B, Tracey A, Corby N, Dunn M, Johnson C, Wood J, Clark S, Pelan S, Griffiths G, Smith M, Glithero R, Howden P, Barker N, Lloyd C, Stevens C, Harley J, Holt K, Panagiotidis G, Lovell J, Beasley H, Henderson C, Gordon D, Auger K, Wright D, Collins J, Raisen C, Dyer L, Leung K, Robertson L, Ambridge K, Leongamornlert D, McGuire S, Gilderthorp R, Griffiths C, Manthravadi D, Nichol S, Barker G, Whitehead S, Kay M, Brown J, Murnane C, Gray E, Humphries M, Sycamore N, Barker D, Saunders D, Wallis J, Babbage A, Hammond S, Mashreghi-Mohammadi M, Barr L, Martin S, Wray P, Ellington A, Matthews N, Ellwood M, Woodmansey R, Clark G, Cooper J, Tromans A, Grafham D, Skuce C, Pandian R, Andrews R, Harrison E, Kimberley A, Garnett J, Fosker N, Hall R, Garner P, Kelly D, Bird C, Palmer S, Gehring I, Berger A, Dooley CM, Ersan-Urun Z, Eser C, Geiger H, Geisler M, Karotki L, Kirn A, Konantz J, Konantz M, Oberlander M, Rudolph-Geiger S, Teucke M, Lanz C, Raddatz G, Osoegawa K, Zhu B, Rapp A, Widaa S, Langford C, Yang F, Schuster SC, Carter NP, Harrow J, Ning Z, Herrero J, Searle SM, Enright A, Geisler R, Plasterk RH, Lee C, Westerfield M, de Jong PJ, Zon LI, Postlethwait JH, Nusslein-Volhard C, Hubbard TJ, Roest Crollius H, Rogers J, Stemple DL. The zebrafish reference genome sequence and its relationship to the human genome. Nature. 2013; 496:498–503. [PubMed: 23594743]

Huang da W, Sherman BT, Lempicki RA. Bioinformatics enrichment tools: paths toward the comprehensive functional analysis of large gene lists. Nucleic Acids Res. 2009a; 37:1–13. [PubMed: 19033363]

Huang da W, Sherman BT, Lempicki RA. Systematic and integrative analysis of large gene lists using DAVID bioinformatics resources. Nat Protoc. 2009b; 4:44–57. [PubMed: 19131956]

Huang H, Du G, Zhang W, Hu J, Wu D, Song L, Xia Y, Wang X. The in vitro estrogenic activities of triclosan and triclocarban. J Appl Toxicol. 2014; 34:1060–1067. [PubMed: 24740835]

Irshad M, Dubey R. Apolipoproteins and their role in different clinical conditions: an overview. Indian J Biochem Biophys. 2005; 42:73–80. [PubMed: 23923565]

Ishibashi H, Matsumura N, Hirano M, Matsuoka M, Shiratsuchi H, Ishibashi Y, Takao Y, Arizono K. Effects of triclosan on the early life stages and reproduction of medaka Oryzias latipes and induction of hepatic vitellogenin. Aquat Toxicol. 2004; 67:167–179. [PubMed: 15003701]

Jacobs MN, Nolan GT, Hood SR. Lignans, bacteriocides and organochlorine compounds activate the human pregnane X receptor (PXR). Toxicol Appl Pharmacol. 2005; 209:123–133. [PubMed: 15885729]

Jung D, Kullak-Ublick GA. Hepatocyte nuclear factor 1 alpha: a key mediator of the effect of bile acids on gene expression. Hepatology. 2003; 37:622–631. [PubMed: 12601360]

Jung EM, An BS, Choi KC, Jeung EB. Potential estrogenic activity of triclosan in the uterus of immature rats and rat pituitary GH3 cells. Toxicol Lett. 2012; 208:142–148. [PubMed: 22062131]

Kerrigan JF, Engstrom DR, Yee D, Sueper C, Erickson PR, Grandbois M, McNeill K, Arnold WA. Quantification of Hydroxylated Polybrominated Diphenyl Ethers (OH-BDEs), Triclosan, and Related Compounds in Freshwater and Coastal Systems. PLoS One. 2015; 10:e0138805. [PubMed: 26466159]

Kimmel CB, Ballard WW, Kimmel SR, Ullmann B, Schilling TF. Stages of embryonic development of the zebrafish. Dev Dyn. 1995; 203:253–310. [PubMed: 8589427]

Kormoczi GF, Saemann MD, Buchta C, Peck-Radosavljevic M, Mayr WR, Schwartz DW, Dunkler D, Spitzauer S, Panzer S. Influence of clinical factors on the haemolysis marker haptoglobin. Eur J Clin Invest. 2006; 36:202–209. [PubMed: 16506966]

Kubota A, Bainy AC, Woodin BR, Goldstone JV, Stegeman JJ. The cytochrome P450 2AA gene cluster in zebrafish (Danio rerio): expression of CYP2AA1 and CYP2AA2 and response to phenobarbital-type inducers. Toxicol Appl Pharmacol. 2013; 272:172–179. [PubMed: 23726801]

Kuehn BM. FDA pushes makers of antimicrobial soap to prove safety and effectiveness. JAMA. 2014; 311:234. [PubMed: 24430309]

Lemon J. Plotrix: A package in the red light district of R. R-News. 2006; 6:8–12.

Li HH, Doiron K, Patterson AD, Gonzalez FJ, Fornace AJ Jr. Identification of serum insulinlike growth factor binding protein 1 as diagnostic biomarker for early-stage alcohol-induced liver disease. J Transl Med. 2013; 11:266. [PubMed: 24152801]

Lorent K, Moore JC, Siekmann AF, Lawson N, Pack M. Reiterative use of the notch signal during zebrafish intrahepatic biliary development. Dev Dyn. 2010; 239:855–864. [PubMed: 20108354]

Louis GW, Hallinger DR, Stoker TE. The effect of triclosan on the uterotrophic response to extended doses of ethinyl estradiol in the weanling rat. Reprod Toxicol. 2013; 36:71–77. [PubMed: 23261820]

Mandrell D, Truong L, Jephson C, Sarker MR, Moore A, Lang C, Simonich MT, Tanguay RL. Automated zebrafish chorion removal and single embryo placement: optimizing throughput of zebrafish developmental toxicity screens. J Lab Autom. 2012; 17:66–74. [PubMed: 22357610]

Marlatt VL, Veldhoen N, Lo BP, Bakker D, Rehaume V, Vallee K, Haberl M, Shang D, van Aggelen GC, Skirrow RC, Elphick JR, Helbing CC. Triclosan exposure alters postembryonic development in a Pacific tree frog (Pseudacris regilla) Amphibian Metamorphosis Assay (TREEMA). Aquat Toxicol. 2013; 126:85–94. [PubMed: 23159728]

Neacsu CD, Ko YP, Tagariello A, Rokenes Karlsen K, Neiss WF, Paulsson M, Wagener R. Matrilin-1 is essential for zebrafish development by facilitating collagen II secretion. J Biol Chem. 2014; 289:1505–1518. [PubMed: 24293366]

Nikolsky Y, Kirillov E, Zuev R, Rakhmatulin E, Nikolskaya T. Functional analysis of OMICs data and small molecule compounds in an integrated “knowledge-based” platform. Methods Mol Biol. 2009; 563:177–196. [PubMed: 19597786]

Noyes PD, Haggard DE, Gonnerman GD, Tanguay RL. Advanced morphological - behavioral test platform reveals neurodevelopmental defects in embryonic zebrafish exposed to comprehensive suite of halogenated and organophosphate flame retardants. Toxicol Sci. 2015; 145:177–195. [PubMed: 25711236]

Oliveira R, Domingues I, Koppe Grisolia C, Soares AM. Effects of triclosan on zebrafish early-life stages and adults. Environ Sci Pollut Res Int. 2009; 16:679–688. [PubMed: 19283420]

Orvos DR, Versteeg DJ, Inauen J, Capdevielle M, Rothenstein A, Cunningham V. Aquatic toxicity of triclosan. Environ Toxicol Chem. 2002; 21:1338–1349. [PubMed: 12109732]

Padilla S, Corum D, Padnos B, Hunter DL, Beam A, Houck KA, Sipes N, Kleinstreuer N, Knudsen T, Dix DJ, Reif DM. Zebrafish developmental screening of the ToxCast Phase I chemical library. Reprod Toxicol. 2012; 33:174–187. [PubMed: 22182468]

Pascual M, Gomez-Lechon MJ, Castell JV, Jover R. ATF5 is a highly abundant liver-enriched transcription factor that cooperates with constitutive androstane receptor in the transactivation of CYP2B6: implications in hepatic stress responses. Drug Metab Dispos. 2008; 36:1063–1072. [PubMed: 18332083]

Paul KB, Hedge JM, Bansal R, Zoeller RT, Peter R, DeVito MJ, Crofton KM. Developmental triclosan exposure decreases maternal, fetal, and early neonatal thyroxine: a dynamic and kinetic evaluation of a putative mode-of-action. Toxicology. 2012; 300:31–45. [PubMed: 22659317]

Paul KB, Hedge JM, Devito MJ, Crofton KM. Developmental triclosan exposure decreases maternal and neonatal thyroxine in rats. Environ Toxicol Chem. 2010a; 29:2840–2844. [PubMed: 20954233]

Paul KB, Hedge JM, DeVito MJ, Crofton KM. Short-term exposure to triclosan decreases thyroxine in vivo via upregulation of hepatic catabolism in Young Long-Evans rats. Toxicol Sci. 2010b; 113:367–379. [PubMed: 19910387]

Paul KB, Thompson JT, Simmons SO, Vanden Heuvel JP, Crofton KM. Evidence for triclosan-induced activation of human and rodent xenobiotic nuclear receptors. Toxicol In Vitro. 2013; 27:2049–2060. [PubMed: 23899473]

Pfaffl MW. A new mathematical model for relative quantification in real-time RT-PCR. Nucleic Acids Research. 2001:29.

Pinto PIS, Guerreiro EM, Power DM. Triclosan interferes with the thyroid axis in the zebrafish (Danio rerio). Toxicol Res-Uk. 2013; 2:60–69.

Pycke BF, Geer LA, Dalloul M, Abulafia O, Jenck AM, Halden RU. Human fetal exposure to triclosan and triclocarban in an urban population from Brooklyn, New York. Environ Sci Technol. 2014; 48:8831–8838. [PubMed: 24971846]

R Core Team, 2013. R: A Language and Environment for Statistical Computing. R Foundation for Statistical Computing. Vienna, Austria:

Ritchie ME, Phipson B, Wu D, Hu Y, Law CW, Shi W, Smyth GK. limma powers differential expression analyses for RNA-sequencing and microarray studies. Nucleic Acids Res. 2015; 43:e47. [PubMed: 25605792]

Rotroff DM, Wetmore BA, Dix DJ, Ferguson SS, Clewell HJ, Houck KA, Lecluyse EL, Andersen ME, Judson RS, Smith CM, Sochaski MA, Kavlock RJ, Boellmann F, Martin MT, Reif DM, Wambaugh JF, Thomas RS. Incorporating human dosimetry and exposure into high-throughput in vitro toxicity screening. Toxicol Sci. 2010; 117:348–358. [PubMed: 20639261]

Schiller V, Wichmann A, Kriehuber R, Schafers C, Fischer R, Fenske M. Transcriptome alterations in zebrafish embryos after exposure to environmental estrogens and anti-androgens can reveal endocrine disruption. Reprod Toxicol. 2013; 42:210–223. [PubMed: 24051129]

Shah SS, Desai HG. Apolipoprotein deficiency and chronic liver disease. J Assoc Physicians India. 2001; 49:274–278. [PubMed: 11225145]

Silver JD, Ritchie ME, Smyth GK. Microarray background correction: maximum likelihood estimation for the normal-exponential convolution. Biostatistics. 2009; 10:352–363. [PubMed: 19068485]

Smyth GK. Linear models and empirical bayes methods for assessing differential expression in microarray experiments. Stat Appl Genet Mol Biol. 2004; 3 Article3.

Solt LA, Kojetin DJ, Burris TP. The REV-ERBs and RORs: molecular links between circadian rhythms and lipid homeostasis. Future Med Chem. 2011; 3:623–638. [PubMed: 21526899]

Song KH, Li T, Chiang JY. A Prospero-related homeodomain protein is a novel co-regulator of hepatocyte nuclear factor 4alpha that regulates the cholesterol 7alpha-hydroxylase gene. J Biol Chem. 2006; 281:10081–10088. [PubMed: 16488887]

Stoker TE, Gibson EK, Zorrilla LM. Triclosan exposure modulates estrogen-dependent responses in the female wistar rat. Toxicol Sci. 2010; 117:45–53. [PubMed: 20562219]

Takeda Y, Jetten AM. Prospero-related homeobox 1 (Prox1) functions as a novel modulator of retinoic acid-related orphan receptors alpha- and gamma-mediated transactivation. Nucleic Acids Res. 2013; 41:6992–7008. [PubMed: 23723244]

Tatarazako N, Ishibashi H, Teshima K, Kishi K, Arizono K. Effects of triclosan on various aquatic organisms. Environ Sci. 2004; 11:133–140. [PubMed: 15746894]

Tilton SC, Siddens LK, Krueger SK, Larkin AJ, Lohr CV, Williams DE, Baird WM, Waters KM. Mechanism-Based Classification of PAH Mixtures to Predict Carcinogenic Potential. Toxicol Sci. 2015; 146:135–145. [PubMed: 25908611]

Tilton SC, Tal TL, Scroggins SM, Franzosa JA, Peterson ES, Tanguay RL, Waters KM. Bioinformatics Resource Manager v2.3: an integrated software environment for systems biology with microRNA and cross-species analysis tools. BMC Bioinformatics. 2012; 13:311. [PubMed: 23174015]

Tolson AH, Wang H. Regulation of drug-metabolizing enzymes by xenobiotic receptors: PXR and CAR. Adv Drug Deliv Rev. 2010; 62:1238–1249. [PubMed: 20727377]

Truong, L.; Harper, SL.; Tanguay, RL. Evaluation of Embryotoxicity Using the Zebrafish Model. In: Gautier, J-C., editor. Drug Safety Evaluation: Methods and Protocols. Totowa, NJ: Humana Press; 2011. p. 271-279.

Truong L, Reif DM, St Mary L, Geier MC, Truong HD, Tanguay RL. Multidimensional in vivo hazard assessment using zebrafish. Toxicol Sci. 2014; 137:212–233. [PubMed: 24136191]

USEPA. ToxCast & Tox21 Summary Files from invitrodb_v2. 2015. pp

Veldhoen N, Skirrow RC, Osachoff H, Wigmore H, Clapson DJ, Gunderson MP, Van Aggelen G, Helbing CC. The bactericidal agent triclosan modulates thyroid hormone-associated gene expression and disrupts postembryonic anuran development. Aquat Toxicol. 2006; 80:217–227. [PubMed: 17011055]

Verstraelen S, Peers B, Maho W, Hollanders K, Remy S, Berckmans P, Covaci A, Witters H. Phenotypic and biomarker evaluation of zebrafish larvae as an alternative model to predict mammalian hepatotoxicity. J Appl Toxicol. 2016

Waters KM, Liu T, Quesenberry RD, Willse AR, Bandyopadhyay S, Kathmann LE, Weber TJ, Smith RD, Wiley HS, Thrall BD. Network analysis of epidermal growth factor signaling using integrated genomic, proteomic and phosphorylation data. PLoS One. 2012; 7:e34515. [PubMed: 22479638]

Wells A, Kopp N, Xu X, O'Brien DR, Yang W, Nehorai A, Adair-Kirk TL, Kopan R, Dougherty JD. The anatomical distribution of genetic associations. Nucleic Acids Res. 2015; 43:10804–10820. [PubMed: 26586807]

Xu X, Wells AB, O'Brien DR, Nehorai A, Dougherty JD. Cell type-specific expression analysis to identify putative cellular mechanisms for neurogenetic disorders. J Neurosci. 2014; 34:1420–1431. [PubMed: 24453331]

Yueh MF, Taniguchi K, Chen SJ, Evans RM, Hammock BD, Karin M, Tukey RH. The commonly used antimicrobial additive triclosan is a liver tumor promoter (vol 111, pg 17200, 2014). P Natl Acad Sci USA. 2015; 112:E237–E237.

Yueh MF, Tukey RH. Triclosan: A Widespread Environmental Toxicant with Many Biological Effects. Annu Rev Pharmacol Toxicol. 2016; 56:251–272. [PubMed: 26738475]

Zhang X, Li C, Gong Z. Development of a convenient in vivo hepatotoxin assay using a transgenic zebrafish line with liver-specific DsRed expression. PLoS One. 2014; 9:e91874. [PubMed: 24626481]

Zorrilla LM, Gibson EK, Jeffay SC, Crofton KM, Setzer WR, Cooper RL, Stoker TE. The effects of triclosan on puberty and thyroid hormones in male Wistar rats. Toxicol Sci. 2009; 107:56–64. [PubMed: 18940961]

Highlights

- Triclosan is a common antimicrobial agent with widespread human exposure.
- Exposure to the triclosan EC_{80} causes robust gene expression changes in zebrafish.
- The liver may be a target organ of triclosan toxicity in embryonic zebrafish.
- Triclosan disrupts normal liver functioning and development in embryonic zebrafish.
- A summary of triclosan's bioactivity profile in the ToxCast program is discussed.

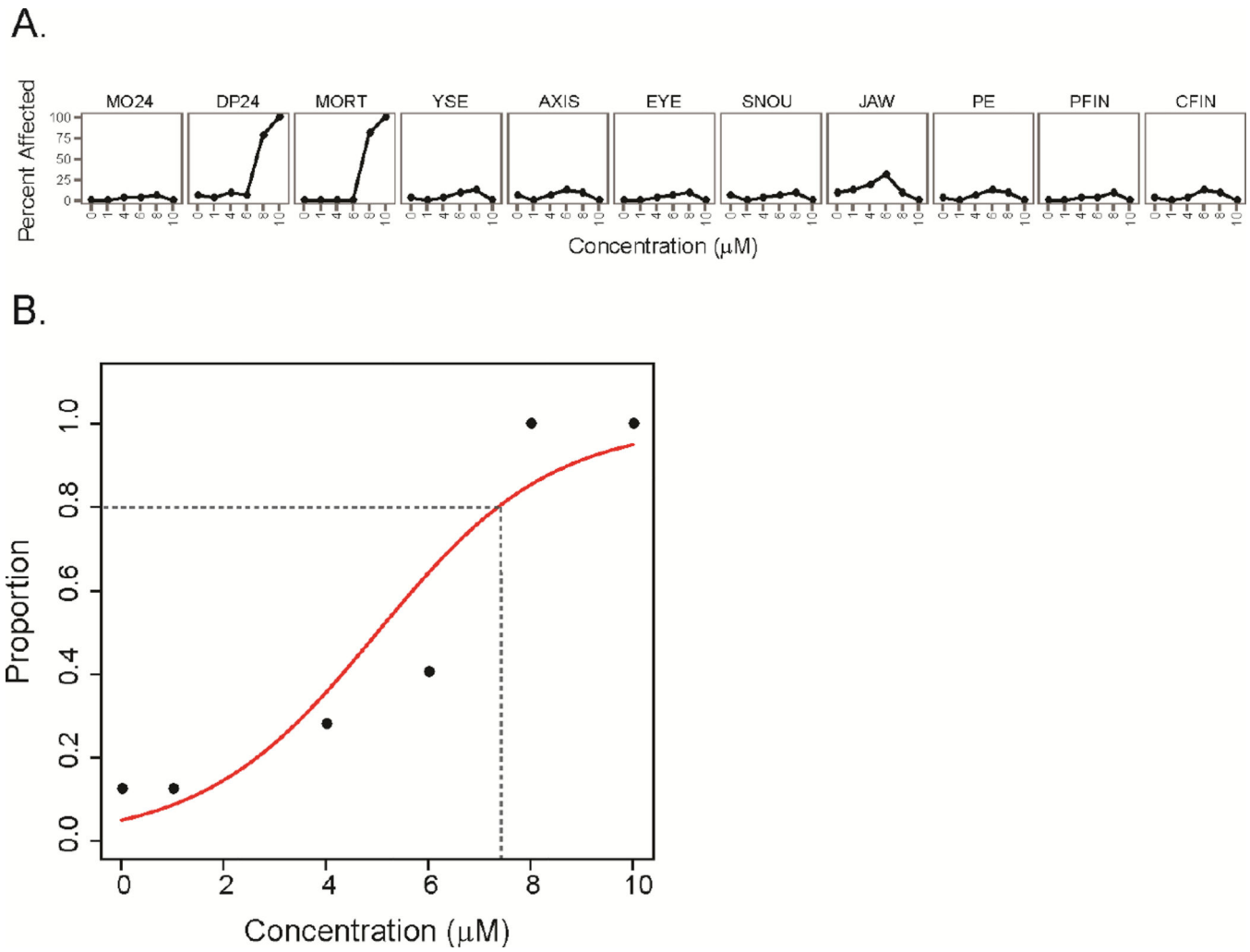

Figure 1.

Developmental toxicity (mortality and morbidity) profile and logistic regression analysis of TCS exposure. (A) Concentration response profile for 0, 1, 4, 6, 8, and 10 μM TCS exposure across 11 phenotypic endpoints. MO24 and DP24 correspond to 24 hpf endpoints, and the remaining correspond to 120 hpf endpoints. (B) Logistic regression analysis of TCS developmental effects for any adverse phenotype, with logistic curve shown in red. Dashed lines indicate the EC_{80}.

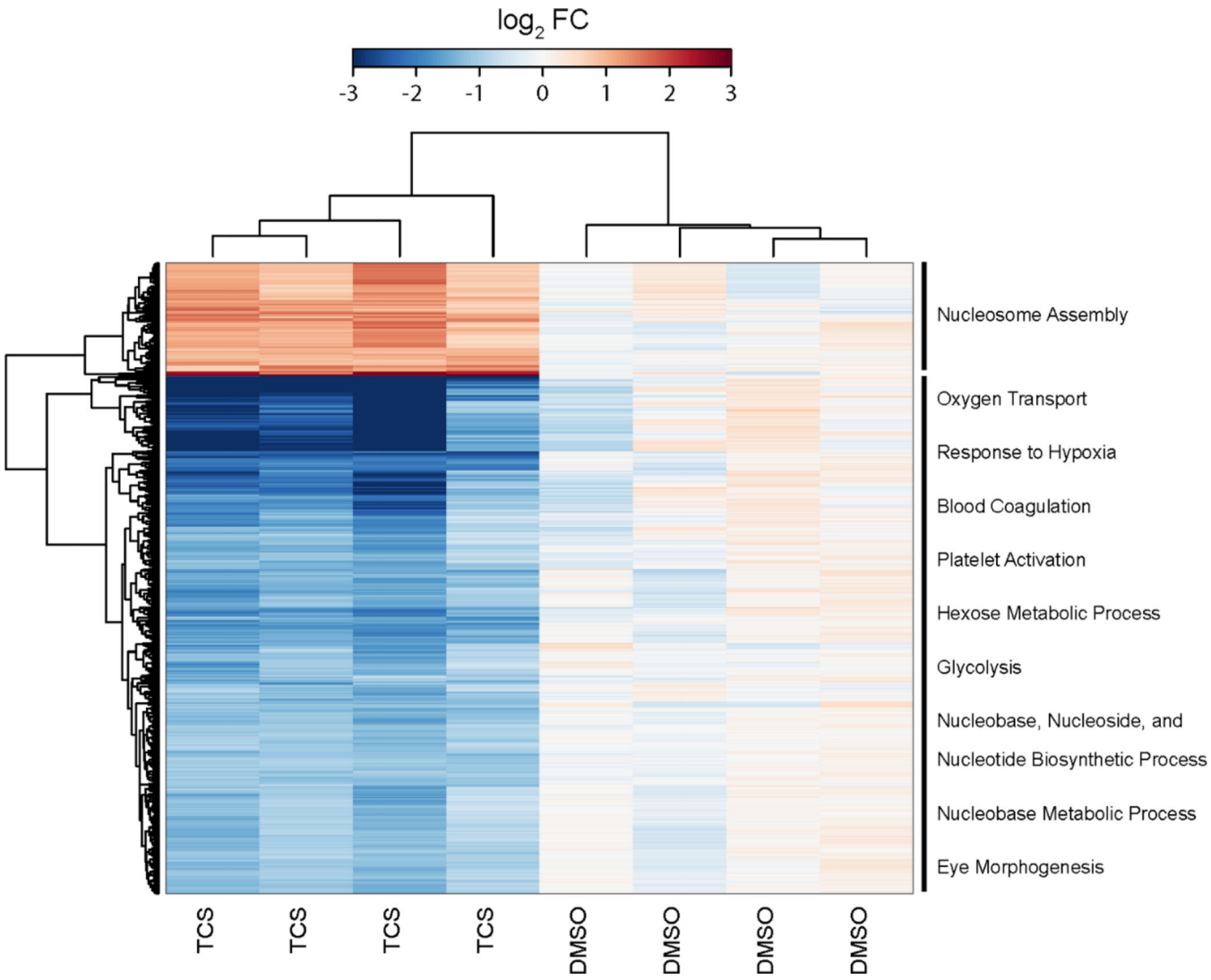

Figure 2.

TCS exposure induces robust transcriptional changes in embryonic zebrafish. Heatmap visualization with bi-hierarchical clustering of significant differentially expressed transcripts due to developmental exposure to the EC_{80} of TCS (FDR corrected p-value ≤ 0.05, fold change ≥ 2.0). The two clusters are annotated by significant functional clusters of enriched GO terms as determined by DAVID.

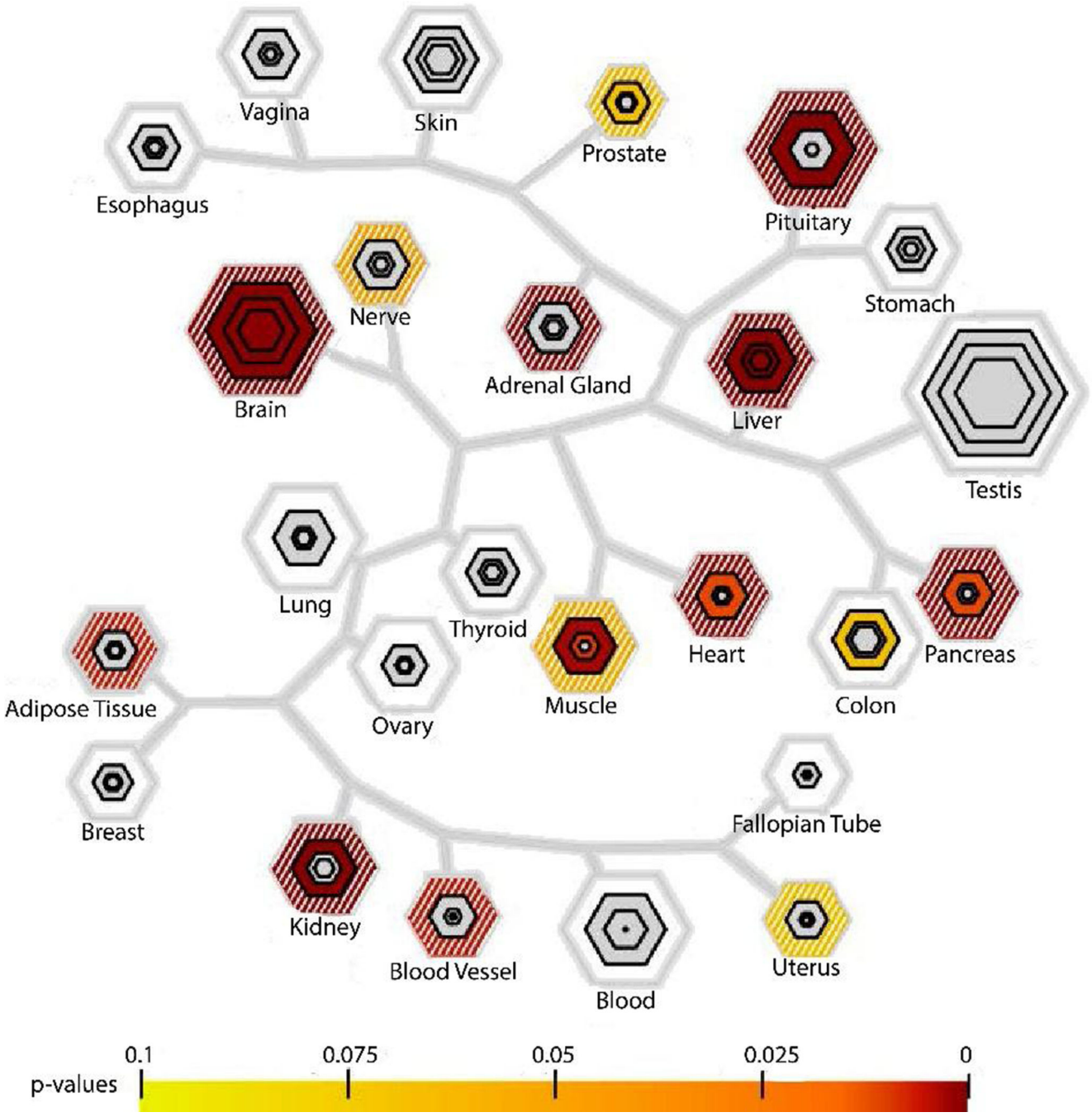

Figure 3.

TCS-induced transcriptional changes are significantly enriched in the liver and brain. Tissue-specific gene enrichment analysis of the significantly differentially expressed orthologous human genes was performed and visualized using the TSEA tool (http://genetics.wustl.edu/jdlab/tsea/). Tissue enrichment are visualized as hexagonal nodes aligned along a dendrogram indicating the similarity of tissue-enriched transcript lists across the 25 tissues.

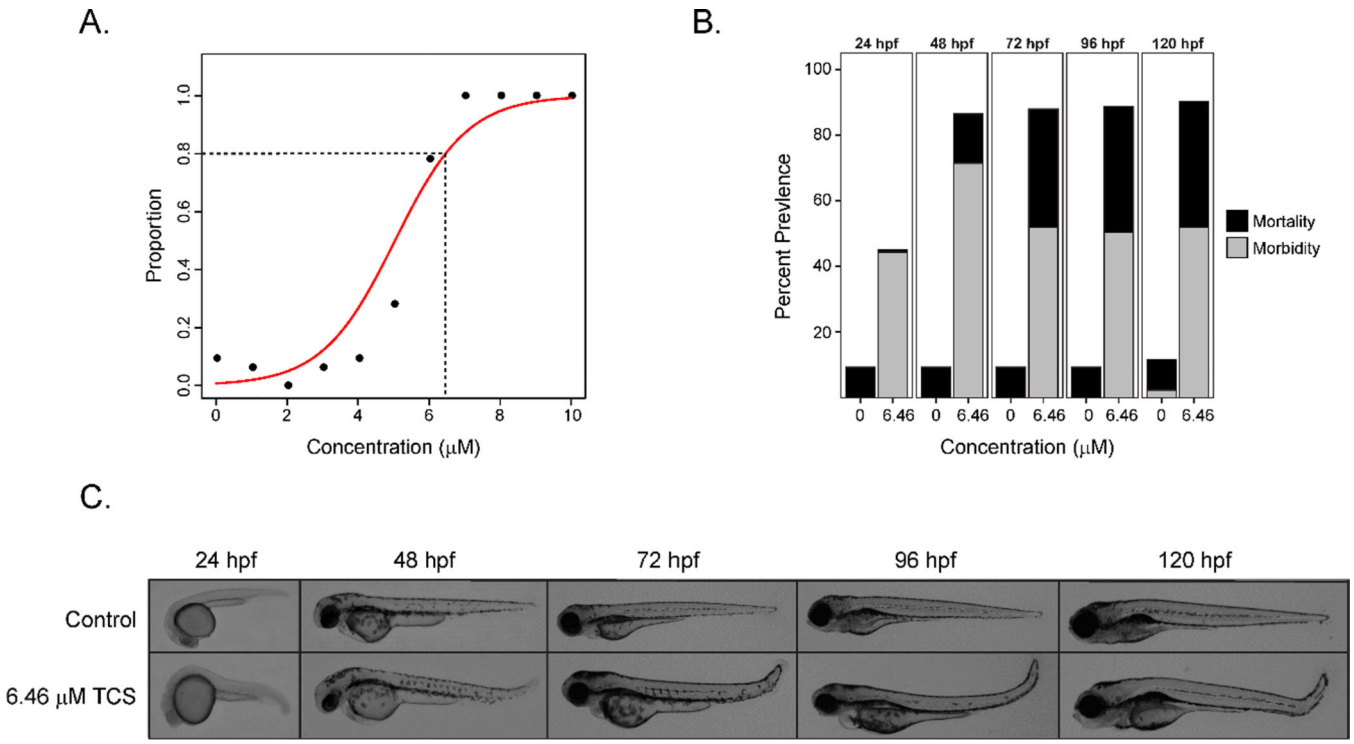

Figure 4.

Developmental time course study of the TCS EC_{80}. (A) Repeated logistic regression analysis for any adverse effect from 0–10 μM of the new TCS stock. Dashed lines indicate the EC_{80}. (B) Percent prevalence for mortality or morbidity at 0 or 6.46 μM TCS at 24, 48, 72, 96, and 120 hpf. (C) Images of zebrafish exposed to 0 (top panel) or 6.46 μM (lower panel) TCS across early development.

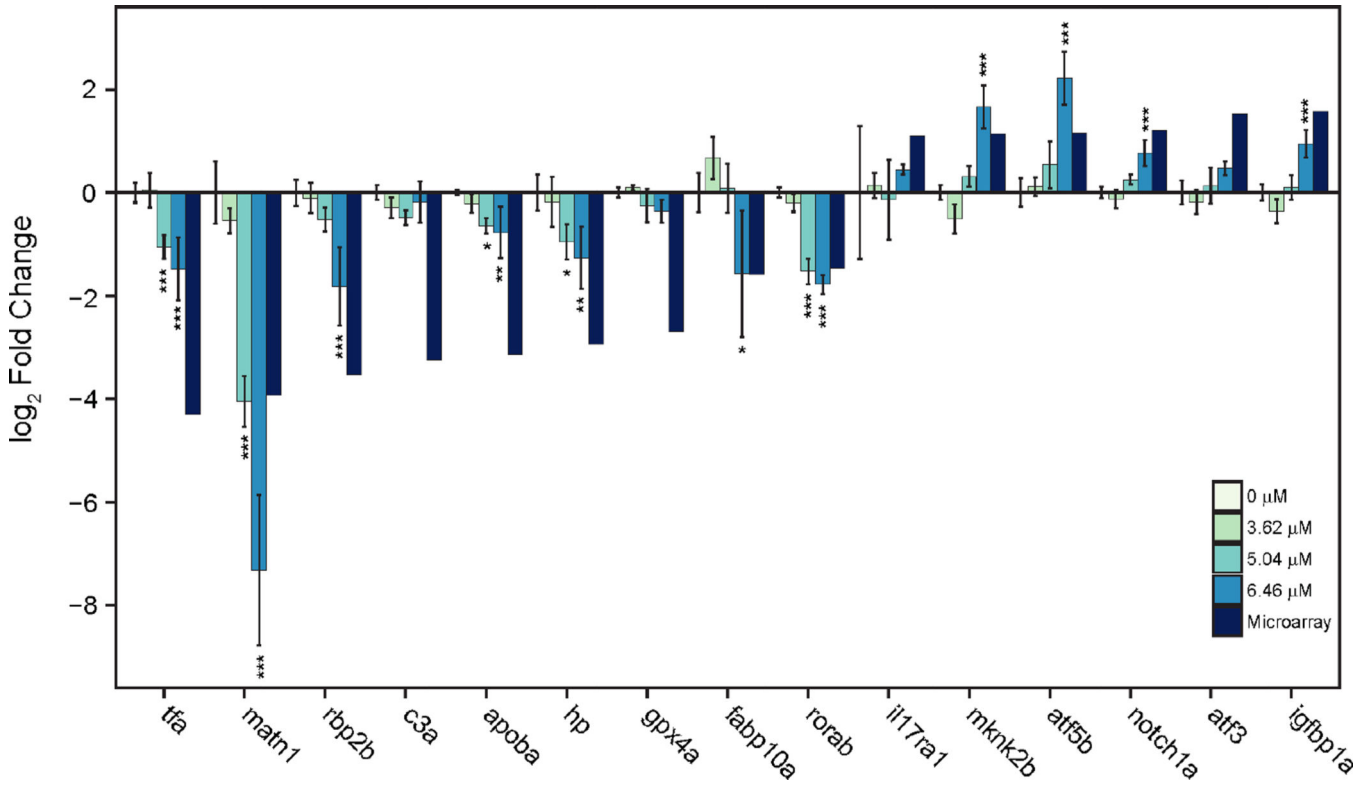

Figure 5.

Quantitative RT-PCR validation of fifteen significantly differentially expressed genes identified in the microarray analysis at the EC_{20}, EC_{50}, and EC_{80} of TCS. log_2 values are shown for comparison between the microarray and qRT-PCR data. A one-way ANOVA with Tukey's post-hoc test or a Kruskal-Wallis with Dunn's post-hoc test were used to test the significance of expression values between qRT-PCR treatment and controls (n=4; * $p \leq 0.05$; ** $p \leq 0.01$; *** $p \leq 0.001$).

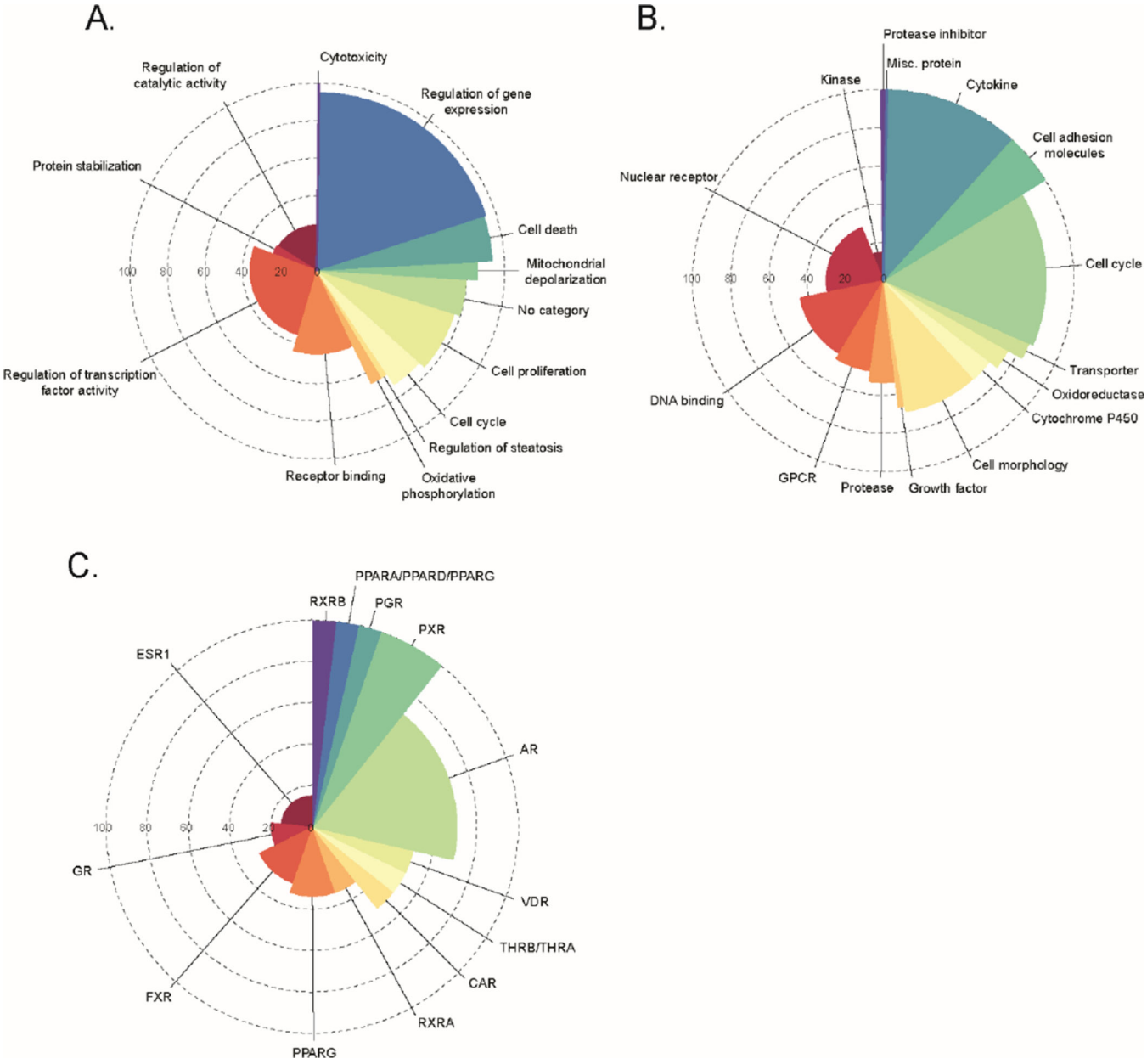

Figure 6.

TCS bioactivity profile across three ToxCast assay annotation levels. Hit-call data across the "biological_process_target" (A), "intended_target_family" (B), and the nuclear receptor subset of "intended_target_family" (C) assay annotation levels were visualized using radial pie diagrams. For reference, the height of a slice indicates the hit percent and the size/angle of the slice indicates the total number of assays within that slice.

Table 1

Significantly enriched MetaCore process networks

Network Name	FDR-adjusted P-value	Associated Human Gene Symbol
Kallikrein-kinin system	9.04E-09	A2M, SERPINC1, KNG1, C3, CPN2, F5, F7, F10, FGA, FGB, FGG, HABP2, SERPIND1, PLAU, SERPINF2, F2
Insulin signaling	1.87E-08	CPE, INS, FBP1, GYS2, PKLR, PFKM, PKM, PYGL, PYGM, SREBF1
Blood coagulation	2.79E-08	A2M, CD9, F10, F2, F5, F7, FGA, FGB, FGG, KNG1, MST1, PLAU, SERPINC1, SERPIND1, SERPINF2, TFPI
Complement system	3.16E-08	C3, C8A, C8B, C8G, C9, CRP, CFHR3, CFHR4, CFH, CFI
IL-6 signaling	1.7E-04	A2M, HBA1, HBA2, BAX, C3, CRP, CP, FGA, FGB, FGG, HABP2, INS, PIK3R3, PIK3R2, SERPINF2
Bile acid regulation of lipid metabolism and negative FXR-dependent regulation of bile acids concentration	2.3E-04	ANGPTL3, APOB, APOE, FBP1, FABP6, INS, PCK1, SREBF1
Visual perception	1.05E-03	ABLIM1, ARR3, CYP1B1, CRYGD, OPN1LW, PDE6H, RAX, RDH11, RGR, RLBP1, RPE65, RCVRN, SIX3
Synaptic vesicle exocytosis	4.9E-02	AMPH, APBA1, DNM1, SEPT5, SLC1A3, SLC6A1, SNAP25, SNCB, STX1B, STXBP1, SV2B, SYT5, VAMP1

Table 2

Statistically enriched transcription factors

Transcription Factor	P-value	Z-score
HNF4α	6.81E-14	9.452
USF1	9.01E-10	8.166
HNF3β	3.39E-09	7.514
HNF1α	9.27E-09	7.382
LHX2	2E-08	6.954
C/EBPα	2.53E-08	6.885
RORα	1.35E-07	7.64
PROX1	3.14E-07	7.929
SP1	3.71E-06	4.944
HNF3α	6.58E-06	5.557
SP3	6.91E-06	5.161
PPARγ	2.04E-05	5.036
LXRa	2.73E-05	5.614
COUP-TFI	3.76E-05	5.6
PPARα	4.89E-05	4.963
USF2	5E-05	5.149